

**UNIVERSITY OF TURKISH AERNAUTICAL ASSOCIATION
INSTITUTE OF SCIENCE AND TECHNOLOGY**

**PERFORMANCE OF POLYMER COATING AND FORMING
CONDITIONS**

**MASTER THESIS
NAJLAA ALQARA GHULI
ID: 1406080030**

**Institute of Science and Technology
Mechanical and Aeronautical Engineering Department
Master Thesis Program**

DECEMBER 2017

**UNIVERSITY OF TURKISH AERNAUTICAL ASSOCIATION INSTITUTE OF
SCIENCE AND TECHNOLOGY**

PERFORMANCE OF POLYMER COATING AND FORMING CONDITIONS

MASTER THESIS

NAJLAA ALOARA GHULI

**IN PARTIAL FULFILLMENT OF THE REQUIREMENT FOR THE
DEGREE OF MASTER OF SCIENCE IN MECHANICAL AND AERONAUTICAL
ENGINEERING**

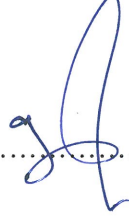
Supervisor: Assist. Prof. Dr. Ibrahim Mahariq

Türk Hava Kurumu Üniversitesi Fen Bilimleri Enstitüsü'nün 1406080030 numaralı Yüksek Lisans öğrencisi "Najlaa Alqara ghuli" ilgili yönetmeliklerin belirlediği gerekli tüm şartları yerine getirdikten sonra hazırladığı "PERFORMANCE OF POLYMER COATING AND FORMING CONDITIONS" başlıklı tezini, aşağıda imzaları bulunan jüri önünde başarı ile sunmuştur.

Tez Danışmanı : Assist. Prof. Dr. Ibrahim Mahariq
Türk Hava Kurumu Üniversitesi

.....


Jüri Üyeleri : Assist. Prof. Dr. Habib Ghanbarpourasl
Türk Hava Kurumu Üniversitesi

.....


: Assist. Prof. Dr. Kerim youde Han
Çankaya Üniversitesi

.....


: Assist. Prof. Dr. Ibrahim Mahariq
Türk Hava Kurumu Üniversitesi

.....


Tez Savunma Tarihi: 29.11.2017

STATEMENT OF NON-PLAGIARISM PAGE

I hereby declare that all information in this document has been obtained and presented in accordance with academic rules and ethical conduct. I also declare that, as required by these rules and conduct, I also declare and certify on my honor that I have fully cited and referenced all the sources I made use of in this present study.



Najlaa Alqara ghuli

29.12.2017

ACKNOWLEDGEMENTS

First of all, I would like to confirm that this work will never be finished without the help of GOD, greater of all creations and the Merciful Prophet Mohammad.

I would like to express my sincere gratitude to my supervisor Assist. Prof. Dr. Ibrahim Mahariq for their patience, guidance and encouragement throughout this work.

I would like to thank all persons who stood beside me and offered their support in one way or another. Finally, I wish to dedicate this thesis to my family, my mother, thank them for encouraging me throughout my studies and other friends for their valuable support.

I would like to express my profound gratitude to my daughters Noor and Narjis, to whom this work is dedicated, for every time they needed me but I wasn't there. For missing me throughout my study.

DECEMBER 2017

NAJLAA ALQARA GHULI

CONTENTS

STATEMENT OF NON-PLAGIARISM PAGE.....	iii
ACKNOWLEDGEMENTS	iv
CONTENTS.....	v
LIST OF TABLES.....	viii
LIST OF FIGURES	ix
ABSTRACT.....	xii
ÖZET	xiv
LIST OF SYMBOLS AND ABBREVIATION.....	xvi
CHAPTER ONE	1
1. INTRODUCTION	1
1.1 Sheet Metal	1
1.2 Advantages of Coated Sheet Metals	3
1.3 Literature Review.....	3
1.3.1 Experimental on Studies uncoated Sheet Metal.....	4
1.3.2 Experimental on Studies Numerical Simulation.....	4
1.3.3 Experiments of Coated Sheet Metals	5
1.3.4 Studies on Fly ash	7
1.4 Contribution of Thesis	8
1.5 Arrangement of Thesis.....	8
CHAPTER TWO	10
2. COATING	10
2.1 Introduction of Coating.....	10
2.2 Method of Coating.....	10
2.2.1. Coil Coating.....	10
2.2.2. Spin Coating.....	12
2.2.3. Physical Vapor Deposition.....	12

2.2.4. Chemical Vapor Deposition.....	12
2.3 Polymer and Polymer Properties.....	13
2.3.1 Epoxy Resin	14
2.3.2 Fly Ash Reinforcing Material	15
2.4 Forming of Sheet Metal	16
2.4.1 Bending	17
2.5 Defects in Coatings during Forming.....	19
2.6 Surface Damage during Forming.....	20
2.6.1 Surface Wear.....	20
CHAPTER THREE.....	22
3. EXPERIMENTAL WORK.....	22
3.1 Experimental part.....	22
3.2 The Used Material.....	24
3.2.1 Epoxy Resin	24
3.2.2 Fly Ash.....	25
3.2.3 Aluminum Alloys.....	26
3.3 Procedure	28
3.3.1 Samples Preparation.....	28
3.3.2 Surface preparation	28
3.3.3 Roughness of the surface	28
3.3.4 Coating Process.....	30
3.4 Mechanical Test.....	33
3.4.1 Tensile Test.....	33
3.4.2. Bending Test	36
3.4.3 Wear Test	38
CHPTTER FOUR.....	39
4. NUMERICAL SIMULATIONS	39
4.1 Interdiction.....	39
4.2 Selections of elements.....	40

4.3 Defining Material Properties.....	41
4.4 Building the Models Geometry.....	42
4.5 Mesh Generation.....	43
4.6 Contact Create.....	44
4.7 Applying the Load and Boundary Conditions	46
CHAPTER FIVE	48
5. REUSLTS AND DISCUSSION	48
5.1 Introduction.....	48
5.2 Tensile Test Results of Used Materials.....	48
5.2.1 Tensile Test results of aluminum alloy	48
5.2.2 Tensile Strength Results of epoxy material.....	49
5.2.3 Tensile Strength Results of epoxy with fly ash.....	49
5.3 Bending Test Results	50
5.3.1 Bending test results of aluminum samples coated without the surface roughness.....	50
5.3.2 Bending results of the aluminum samples coated with the surface roughness	55
5.4 Drop Test	64
CHAPTER SIX	69
6. CONCLUSION AND RECOMMENDATION	69
6.1 Conclusions.....	69
6.2 Recommendations for Forthcoming Work	70
REFERENCES	71

LIST OF TABLES

Tables

Table 2. 1: General mechanical characteristic of epoxy resin	15
Table 2. 2: Physical properties of the fly ash	16
Table 3. 1: Characteristic of epoxy used in this work according to the properties of Product Company which depended on the ASTM	24
Table 3. 2: The chemical composition analysis of fly ash Nanoparticles	25
Table 3. 3: Chemical composition of Aluminum alloy	27
Table 3. 4: Surface roughens values in μm units	29
Table 3. 5: Epoxy resin with fly ash ratios	31
Table 5. 1: Mechanical properties for Aluminum alloy	49
Table 5. 2: Mechanical properties for epoxy resin	49
Table 5. 3: The results of tensile strength after the addition of different Fly ash ratios ...	50
Table 5. 4: The maximum elongation at break (mm) in experimental and simulation tests.	52
Table 5. 5: The maximum Elongation (mm) in the experimental and simulation test of the samples (B1, B2, B3 and B4) with roughness (100 grit)	57
Table 5. 6: The maximum Elongation (mm) in the experimental and simulation tests of the samples with roughness (320 grit)	59
Table 5. 7: The maximum Elongation (mm) in the experimental and simulation tests of the samples with roughness (600 grit)	62
Table 5. 8: The properties of the steel ball	65

LIST OF FIGURES

Figures

Figure 1. 1: Sheet Metal.....	2
Figure 2. 1: Coil coating process.	11
Figure 2. 2: Typical build-up of a coil paint coating	11
Figure 2. 3: Spin Coating	12
Figure 2. 4: Variation in the colors of fly ash.	16
Figure 2. 5: Some of bending types	19
Figure 2. 6: Testing of a rectangular bar under a) three-point bend b) The deflection obtained by bending	19
Figure 2. 7: Deficiencies in Coating	20
Figure 3. 1: Flow chart of experimental work steps.	23
Figure 3. 2: Epoxy resin and hardener.	24
Figure 3. 3: Fly ash powder	25
Figure 3. 4: Spectrometer device	26
Figure 3. 5: Microstructures to the aluminum at 100 x magnification b) sample of aluminum alloy.	26
Figure 3. 6: Optical Microscope	27
Figure 3. 7: Roughness surface device	29
Figure 3. 8: Samples of roughness surface test.....	29
Figure 3. 9: Some of aluminum alloy samples, a) before coating b) after coating	30
Figure 3. 10: Electronic balance.	31
Figure 3. 11: The method of mixing the epoxy with fly ash.....	32
Figure 3. 12: Aluminum alloy specimens a) before coating b) after coating.	32
Figure 3. 13: Samples of tensile test.	33
Figure 3. 14: Tensile test standard specimen.	34
Figure 3. 15: Experimental specimens test.	34
Figure 3. 16: Sample of tensile test (epoxy resin).	35
Figure 3. 17: Tensile test standard specimen.	35
Figure 3. 18: Three- point bending test (simple specimen).	36
Figure 3. 19: Specimens after bending.	36
Figure 3. 20: Bending machine	37
Figure 3. 21: Samples of epoxy resin a) before testing b) next testing.....	37
Figure 3. 22: Wear test device.	38
Figure 4. 1: Flow chart of the analysis procedure.....	40

Figure 4. 2: Solid 185 Homogeneous Structural Solid Geometry.	41
Figure 4. 3: The part in 3D model of aluminum alloy sample.....	42
Figure 4. 4: The part in 3D model of aluminum alloy coated by epoxy resin.	43
Figure 4. 5: Mesh Generation for Aluminum alloy coated by epoxy resin.	43
Figure 4. 6: CONTA174 Geometry	45
Figure 4. 7: TARGE170 Geometry.....	45
Figure 4. 8: Define load applying	46
Figure 4. 9: Define Boundary Condition.	47
Figure 5. 1: The relationship between tensile strength and percentages weight of fly ash powder additives.	50
Figure 5. 2: The flexural strength of aluminum coated as a function of wt. % of fly ash content in the epoxy coating layer without surface roughness surface.....	51
Figure 5. 3: The maximum shear stress of aluminum coated as a function of wt. % of fly ash content in the epoxy coating layer without surface roughness.....	51
Figure 5. 4: Comparison the elongation (mm) of aluminum alloy samples (A1, A2, A3 and A4) coated by polymer without surface roughness of product in the numerical and experimental tests	53
Figure 5. 5: (a,b,c and d) shows elongation at break in aluminum alloy coated by epoxy with different weight percentages of fly ash under bending test in the numerical simulation	54
Figure 5. 6: The flexural strength of aluminum samples coated as a function of the surface roughness content in the epoxy coating layer with variation ratios of fly ash	55
Figure 5. 7: Maximum shear strength of aluminum samples coated as a function of the surface roughness content in the epoxy coating layer with (wt. % of fly ash).....	56
Figure 5. 8: Comparison between numerical and experimental elongation (mm) of the (B1, B2, and B3and B4) samples	57
Figure 5. 9: (a,b,c and d) shows the elongation in the aluminum alloy coated by epoxy with different wt% of fly ash under bending test in numerical analysis	59
Figure 5. 10: Comparison between numerical and experimental to the elongation (mm) of the (C1, C2, and C3and C4) samples.....	60
Figure 5. 11: (a,b,c and d) shows elongation in aluminum alloy coated by epoxy with different wt% of fly ash under bending test by using the numerical analysis.....	61
Figure 5. 12: Comparison between numerical and experimental elongation (mm) of the (D1, D2, and D3and D4) samples.....	62

Figure 5. 13: (a,b,c and d) shows the elongation in the aluminum alloy coated by epoxy with differant wt% of fly ash under bending test by using the numerical analysis.....	64
Figure 5. 14: The model of Drop test.....	65
Figure 5. 15: Drop test of Aluminum alloy coated by epoxy.	66
Figure 5. 16: Drop test of Aluminum alloy coated by epoxy with 1% fly ash.....	67
Figure 5. 17: Drop test of Aluminum alloy coated by epoxy with 2% fly ash.....	67
Figure 5. 18: Drop test of Aluminum alloy coated by epoxy with 3% fly ash.....	68

ABSTRACT

Performance of Polymer Coating and Forming Conditions

NAJLAA ALQARA GHULI

Master, Department of Aeronautics and Mechanical Engineering

Supervisor: Assist. Prof. Dr. Ibrahim Mahariq

December 2017, 74 Pages

Abstract:

Coated sheet metal being environment friendly and cost effective as compared to uncoated sheet metal, are widely used in construction, packaging, transportation and automotive industries. During forming process, major surface damage occurs when the coated sheet is bent or unbent. Therefore, proper control of the parameters during forming and detail study of the surface conditions is required. This work presents a study of performance of polymer coating to aluminum alloy, by the use of epoxy resin with fly ash at different ratios as a reinforcement material and the effect on the mechanical properties (tensile properties, bending properties and drop test) of the polymer coating to help the designer to make better and stronger polymer coating. This study includes experimental and numerical parts in this research, the elongation of different samples is evaluated at different values of fly ash powder. Sixteen samples of aluminum sheet metals were prepared by laboratory proses to study the effects of nanoparticle ingredients on the polymer coating interface, four specimens without surface roughness, and the other samples with surface roughness were coated by epoxy resin with variations of fly ash powder.

The F.E.M was applied using (ANSYS VR .15) software package in order to determine the optimum value of the deformation on the coating surface which can satisfy

the objectives of this work and reduce efforts, time and costs. A 3D model was built, exploiting the plane strain condition for bending test.

The results obtained from the experimental work show the tensile strength and elongation at break of nano composite material increased gradually with increasing the weight percentage of fly ash powder from 0 wt.% to 3 wt. % fly ash, While, the flexural strength and maximum shear strength decreases with increase in fly ash content and increase in the surface roughness.. The differences in results between the experiments and numerical analysis are small, and that indicates to success of the program followed in the experimental and simulation procedures therefore, a program can be adopted for other tests, Drop Test, It is one of these of practical experiments. It is convenient to use ANSYS with assumptions of using a steel ball to conflict the painted side of sample to study the speed of hitting with the coated layer before and after addition of fly ash in previously mentioned ratios, the result show the impact velocity decrease in fly ash ratio increase.

ÖZET

Şekillendirme Koşulları Ve Polimer Kaplamalarının Performansı

NAJLA ALQARA GHULI

Yüksek Lisans Tezi, Makine Mühendisliği Anabilim Dalı

Tez Danışmanı: Yrd. Doç. Dr. İbrahim Mahariq

Aralık 2017, 74 sayfa

Özet:

Kaplamasız sac metal ile karşılaştırıldığında çevre dostu ve uygun maliyetli olan kaplamalı sac, inşaat, ambalajlama, taşıma ve otomotiv endüstrilerinde yaygın olarak kullanılmaktadır. Şekillendirme işlemi sırasında, kaplamalı sac büküldüğünde veya düzeltildiğinde büyük yüzey hasarları oluşur. Bu nedenle, şekillendirme esnasında parametrelerin düzgün kontrolü ve yüzey koşullarının ayrıntılı olarak incelenmesi gereklidir. Bu araştırmada tasarımcıya daha iyi ve daha güçlü bir polimer kaplama yapmasına yardımcı olmak amacıyla uçucu kül ile epoksi reçinenin farklı oranlarda güçlendirme malzemesi olarak kullanılması ile polimer kaplamanın alüminyum alaşımına uygulanması ve polimer kaplamanın mekanik özellikleri (gerilme özellikleri, eğilme özellikleri ve düşme testi) üzerindeki etkisi sunulmaktadır. Bu çalışma, araştırmadaki deneysel ve sayısal kısımları içermekte olup, farklı numunelerin elongasyonu uçucu kül tozunun farklı değerlerinde değerlendirilmektedir. Nano-parçacık bileşenlerinin polimer kaplama ara yüzü üzerindeki etkilerini görmek için laboratuvar süreçleri ile on altı alüminyum sac metal numunesi hazırlanmış olup, yüzey pürüzlülüğü olmayan dört numune ve yüzey pürüzlülüğüne sahip diğer numuneler uçucu kül tozu çeşitleri ile epoksi reçinesi ile kaplanmıştır.

Kaplama yüzeyindeki deformasyonların optimum değerlerini belirlemek için çalışmanın hedefleri yerine getirecek ve zaman, çaba ve maliyeti azaltacak olan (ANSYS VR .15) yazılım paketi kullanılarak F.E.M uygulanmıştır. Eğilme testi için düzlem gerilme şartını kullanan bir 3D model oluşturulmuştur.

Deneysel alıřmadan elde edilen sonular, uucu kl tozunun aėırlık yzdesinin aėırlıka % 0 'dan % 3'e ykseltilmesi ile nano kompozit malzemenin kopma noktasındaki gerilme mukavemeti ve uzamasının yavařa arttıėını bununla birlikte uucu kl miktarı ve yzey przllėindeki artıřla eėilme mukavemeti ve maksimum kesilme mukavemetinin azaldıėını gstermiřtir. Deneysel ve sayısal analizler arasındaki sonu farklılıkları kktr, bu da deneysel ve simlasyon srelerinde uygulanan programın bařarısını gstermektedir. Bu nedenle, program diėer testlere de uyarlanabilir. Dřme Testi, deney pratiklerinden birisidir. Daha nce bahsedilen oranlarda uucu kl ilavesinden nce ve sonra kaplanmış katman ile arpma hızını incelemek iin numunenin boyalı tarafına arpıtırma amacı ile elik bilyanın kullanılması varsayımı ile ANSYS kullanılması uygundur, sonular arpma hızının uucu kl oranı artıřı ile dřtėn gstermektedir.

LIST OF SYMBOLS AND ABBREVIATION

Symbols	Meaning
AFM	Atomic Force Microscopy
ASTM	American Society for Testing and Materials
COF	Coefficient of Friction
CRTD	The Critical Ratio of Coating Thickness to Indentation Depth
CVD	Chemical Vapor Deposition
EIS	Electrochemical Impedance Spectroscopy
FEM	Finite Element Method
PVD	Physical Vapor Deposition
SEM	Scanning Electron Microscopy
SMF	Sheet Metal Forming
TEM	Transmission Electron Microscopy
TOM	Transmission Optical Microscopy
VTES	Vinyl Tri Ethoxy Silane
Y_c/Y_s	The Yield Strength Ratio of Coating to Substrate
Abbreviation	Meaning
Al_2O_3	Aluminum oxide
CeO	Calcium Oxide
Fe_2O_3	Iron oxide
K_2O	Potassium Oxide

MgO	Magnesium Oxide
Na ₂ O	Sodium Oxide
NaOH	hydroxide sodiu
SiO ₂	Nano silica oxide
SO ₃ ,	Sulfur Oxide
TiC	Titanium Carbide
TiO ₂	Nano titanium oxide
ZnO	Zinc Oxide
ZrO ₂	Nano zirconium oxide

CHAPTER ONE

INTRODUCTION

1.1 Sheet Metal

Metal Sheet is formed by an industrial procedure into thin, flat pieces. It is one of a critical forms used in metal working and it be able to cut and bent into a range of shapes. Everyday countless things are made-up from metal sheet. Thicknesses can vary considerably; very thin sheets are considered foil or leaf, and parts thicker than 6 mm are considered plate [1].

There are several different metals can be made into metal sheet, such as aluminum, steel, tin, copper, titanium, brass, and nickel as shown in Figure 1.1.

The coated sheet metal is widely used in automotive, construction, transportation, decorative, consumer products and packaging manufacturing. The surface of these sheets is painted with different paint systems which provide glossy and shiny decorative surface finish and protection against corrosion. Also, sheet metals which are mostly used in major industries due to their high flexibility and numerous ranges of mechanical strengths compared to other materials, such as polymers or ceramics [2].

It is well known that the aluminum in these days the best broadly used metallic material beside steel. The exceptional combinations of properties providing by aluminum and its alloys make aluminum the greatest versatile, inexpensive, and attractive metallic materials for a wide variety of uses from soft, highly elastic wrapping foil to the most demanding engineering applications [3].

The mechanical features of aluminum compromise an increasing solicitation field, specifically where lightweight constructions are required [4].

The demands for enhanced characteristics, such as better durability, the excellent mechanical, higher strength, chemical (i.e., corrosion and degradation) make aluminum attractive in spite of its poor thermal properties. Associated to polymers and wood, metals have a significantly higher thermal conductivity.

Coated aluminum metal sheet is widely used for building applications in products as roof; facade shutters sections, and blinds, door and window over a broad range of wave lengths, leading to its collection for a variety of decorative and functional uses [5].

Also, for its good electrical conductivity, aluminum sheets are widely used in low tension insulated with epoxy windings of distribution transformers.

In metal sheet forming, the parameters can be divided into main groups:

- 1- Geometric parameters contain the surface characteristics of the work piece.
- 2- Process parameters include the typical force, bending test and tension test.
- 3- Control of these parameters will give very smooth surface on the finishing product without any trace of surface wear.
- 4- Study of those parameters will give an improved understanding of the causes and reason for surface damage. Whereas, study of polymer coated sheets was mostly related to the surface damage and properties of coatings under loads normal to the surface. The performance of an engineering piece is limited by the properties of the material which have been prepared and to stipulate the material used [6].



Figure 1. 1: Sheet Metal [2]

1.2 Advantages of Coated Sheet Metals

Coated sheet metals have various advantages over uncoated sheet metal, they boost efficiency, lessen processing cost and provide better quality products. The other unique advantages offered by them are: [7]

1. Corrosion protection to metallic sheets and higher resistance characteristic against different harsh weathers.
2. They act as dry lubricants in the forming process. This eradicates and eliminates the need of using lubricants and increases the formability of metal sheets.
3. Coated sheet metals eliminate the need for wash, coat, spray and are free of rutted application or defects on the surface due to the same. They are also free from dirt or any other residuals and particles on the surface.
4. As they eliminate organic compounds emissions (there is no remedial process), coated sheet metals are eco-friendly.
5. Forming of coated sheet metal is less time consuming and an energy efficient procedure. They have less transportation, storage and production cost and more energy effluent when compared to the conventional spraying methods.
6. Coated sheet metal provides shiny and aesthetic finish to the surface.

1.3 Literature Review

In literature, there have been many researchers involved the surface damage which is depended on various parameters. For this reason, materials selection is a duty usually carried out by design and materials engineers. The objective of materials selection as the identification of materials, which after appropriate industrial operations, will have the properties needed for the product or component to demonstrate it is required function at the lowest cost. Free-form manufacture is a very encouraging technology due to the efficient and simple process for creating microstructures [8].

For the purpose of material choice, thousands of data would be wanted to characterize all the grades of materials. Many selection techniques are accessible to help design engineers to choose the most suitable materials.

1.3.1 Experimental on Studies uncoated Sheet Metal

To illustrate that, P. Saha [9] conducted friction experiments on uncoated sheets metals using bending under tension test. The experimental set up was done to measure the force during forming. First set of experiments were directed by electro-galvanized steel sheets on a smooth die steel and another set of research with greased 1100 H-14 aluminum on a smooth cemented carbide. Author are studied the effect of friction coefficient through the forming process, contact pressure, plastic strain and strain rate. COF with plastic strain was found to depend on the features of material, so the material that has more dispositions to roughen with plastic strain founded decreased the COF, while the material that has less dispositions to roughen showed high COF.

A. Azushima and M. Sakuramoto. [10]. Studied the mechanical properties, contact pressure, roughness of surface and COF. The specimen used was A1100 aluminum sheet of dimensions (500 × 10 × 1) mm (L × W × T). The die used is made of tool steel, and the paraffin basically oil was used as lubricant. The surface roughness was measured by contact needle type roughness meter, and the elongation was measured by using scribed pattern on the sample. When the contact pressure was less, the roughness of surface decreased while the roughness of surface increased at higher contact pressure, and COF decreased.

1.3.2 Experimental on Studies Numerical Simulation

Experimental analysis was extended to numerical simulations. Numerical simulation was employed to find the relation among various parameters used in the process.

N. Panich, et al. [11], conducted a study to simulate Nano indentation of mushy coatings on hard substrates using Finite element method. The climacteric ratio of coating thickness to indentation depth (CRTD) in terms of yield strength ratio and indenter tip radius was investigated using FEM.

Simulations were carried out for different tip radio of indenter ranging from $r = 0, 0.2, 0.5, 1$ and 2 mm. The thickness of the coating was considered to be 1micrometer. Therefore, the indentation process has a large influence by the indenter tip radius. On increasing the tip radius, the critical indentation depth decreases (CRTD increases).The yield strength proportion of coating to substrate was also seen to have a large effect on the CRTD, and by increasing Y_c/Y_s (making the coat harder), the critical indentation depth was observed to decrease. Based

on the FEA results, an equation was modeled which would give the critical indentation depth where the substrate effect is just 5 percent. The critical indentation depth was seen to be dependent on structure of the coatings, brittleness of hard coatings, the tip radius of indenter and the yield strength ratio of coatings and substrate.

In Ref. [12], investigation the simplicity of the test is the pencil hardness test, which is most recurrently used in industries to characterize the hardness of the coatings. Other tests include ford- five- finger test, pin-on-disc test, taber test, needle test and scratch apparatus. The several factors that effect on the scratch behavior of polymers are the scratch speed, load on the surface and the fillers present in the material. A stainless steel ball with a diameter of 1 mm was used as a scuff stylus tip for a scratch length of 100 mm. Four different Polypropylene material systems were used. They are homopolymers and copolymers with no talc and talc (20% by wt.) rollers. After experimentation, (Transmission optical microscopy) TOM, SEM and scanned images were used to study a damage of surface. Finite element analyses were conceded out using FEM/Explicit. A 3D model was created. Scratch resistance was experimentally to be more in homopolymer when related to copolymer. The result of coating ductility and coating depth on the scratch resistance was found that coating with higher ductility appeared better adhesion than the coating with lower ductility. Thus, the results suggested a critical coating thickness to minimize the damage.

1.3.3 Experiments of Coated Sheet Metals

There are broadly uses of polymers in food packaging, aerospace, automobile, coatings and microelectronic packaging industries, a lot of work was done in past to evaluate the properties of polymers and the performance of polymers under various conditions .

In Ref [13], work was done to examine an influence of surface roughness and the indenter tip radius on the scratch resistance at polymer. Nano scratch tests were conducted by Dynamic Nano mechanical probe system. Experiments were conducted on thermoplastics and thermoset materials. Under constant load and scratch rate testing condition, it was observed that the surface roughness had no or very little effect at the surface damage of a polymer, whereas the surface damage was found to be material specific. In Nano scratch testing, the higher modulus was advantageous while for micro scratch testing, this might lead to higher stresses.

The results showed the influence of indenter tip radius on the surface damage of the polymer. Scratch penetration and stress increased by increasing the indenter tip.

J. B. Bajata et al. [14], in this study, the electrochemical and transport properties and adhesion of epoxy coatings electrodeposited on aluminum pretreated by (vinyltriethoxysilane VTES) were investigated through exposure to 3% NaCl. The VTES layers were deposited on aluminum surface from 2% and 5% vinyltriethoxysilane solution. The electrochemical effects showed that the pretreatment based on VTES film deposited from 5% solution provides enhanced barrier properties and excellent corrosion armor. The amount of diffusion coefficient of water through epoxy coating on this substrate and water content inside the epoxy coating were the smallest, indicating the low porosity of the coating. In addition, the worthy adhesion was maintained throughout the whole investigated time period.

Toshiyasu. N and Vedarajan. R [15]. Aluminum nanoparticles were coated by epoxy polymer in order to prevent the corrosion response. The coverage of the epoxy polymer film was measured from 0% to 100%, which changed the corrosion rate of nanoparticles quantitatively. The surface of a polymer coating was investigated by transmission electron microscopy (TEM) and atomic force microscopy (AFM), and the corrosion resistance of these nanoparticles was calculated by the wet/dry corrosion test on platinum plate with a NaCl solution. From a TEM analysis, 10 mass% polymer-coated Al particles in the synthesis were practically 100% covered on the surface by a polymer thin layer of 10 nm thick. On the other hand, 3 mass% polymer-coated Al was partially covered by a film. In the AFM–Kelvin force microscopy; this indicated that the conductivity of the Al was isolated from Pt plate by the polymer.

Tullio. M et al. [16]. This study investigation the use of graphene as a conductive nanofiller in the forthcoming of inorganic/polymer nanocomposites has attracted increasing interest in the aerospace arena. In this work, graphene nanoflakes were incorporated into a water-based epoxy resin, and then the hybrid coating was applied to Al 2024-T3 samples. The adding of graphene considerably improved some physical properties of the hybrid coating as demonstrated by (EIS) analysis, ameliorating anti-corrosion performances of raw material. The use of graphene as a conductive nanofiller in the preparation of inorganic/polymer nanocomposites has attracted increasing concentration in the aerospace field and graphene is an

ideal candidate to enhance the anti-corrosion properties of the resin, since it absorbs most of the bright and provides hydrophobicity for repelling water.

Amer. H. Majeed et al. [17], in this work, graphene nanoflakes were incorporated into a water-based epoxy resin, and then the hybrid coating was utilized to Al 2024-T3 samples. The raise of graphene considerably improved some physical properties of the hybrid coating as demonstrated by Electrochemical Impedance Spectroscopy analysis, ameliorating anti-corrosion performances of raw material. The nanocomposites were ready with (1 to 10 wt. %) of carbon black nanoparticles using ultrasonic surge bath machine dispersion method. The results had displayed that the tensile strength, tensile modulus of elasticity, flexural strength and impact strength are improved by (24.02%, 7.93%, 17.3% and 6%) respectively at 2wt %. Hardness and the compressive strength are improved by (12%, 44.4%) at 4wt%.

1.3.4 Studies on Fly ash

A. Pattanaik1 et al. [18], investigation in the research work, fly ash is added to four diverse weight percentages compositions and post-curing has been done in the atmospheric situation, micro oven and, normal oven. Tests were carried out on the developed polymer composite to measure its dielectric permittivity and tan delta value in a frequency range of 1 Hz - 1 MHz. The dielectric strength and losses are compared for changed conditions. Post curing increases the crystallinity of the complex which increases the mechanical strength of the material, Dielectric constant of fly ash epoxy composite decreases with increase in rate. Dielectric strength increases with post curing conditions. Dielectric constant decreases with increase in % reinforcement of fly ash. Fly ash epoxy polymer composite can be used in electronics industries electrical as a good dielectric material.

Nityananda. K. [19] described the development of epoxy based composites with the amalgamation of fly ash, an industrial waste, as reinforcement. In coal based thermal power plants fly ash is produced throughout power generation. Five different volume fractions (0, 5, 10, 15 and 20% fly ash) were used in this study to synthesis the epoxy-fly ash composites. Effect of fly ash pleased on the mechanical properties of these composites underneath different mechanical test conditions was studied in a comprehensive way. The results suggested that compressive strength and the tensile of these composites increases with increasing fly ash

content while the flexural strength and the impact strength decreases with increase in fly ash gratified. Detailed microscopic observations were carried out for all fractured surfaces.

1.4 Contribution of Thesis

To avoid painting of sheet metal of post forming, continuous coating is at first applied on sheet metal followed by a forming procedure to obtain a desired shape, and reduce the deformation of polymer coating by improving performance characteristics of coated sheet metal by using (epoxy resin) as a polymer coating, also, studying the effect of adding fly ash in variation values to (epoxy resin), and it is effect on adhesive force. Also in the present study, properties of polymer coatings will be noticed using bending test, tension test, and surface roughness.

The other purpose of the present study is to conduct a simulation between the experimental score and the results obtained from numerical simulations to analyze.

The present work is divided into three major parts:

1. Building an experimental set-up to simulate the real forming process.
2. Conducting experiments and records analysis.
3. Conducting numerical simulations to analyze the specimens in various testing conditions.

1.5 Arrangement of Thesis

The repose of the chapters in this thesis arranged as follows:

Chapter one. In this chapter, introduction of sheet metal, advantages of coated sheet metal, and the literature are presented. Contribution of thesis and arrangement of thesis are also illustrated.

Chapter two. Describes the introduction of coating, method of coating, polymer properties, forming of sheet metal, defects in coatings during forming and Surface damage during Forming.

Chapter three .Introduces a detailed description of the experimental methodology is presented, which includes materials selection, sample preparation methods and detailed description of test instruments used as well as specimens images before and after the examination.

Chapter four. Describes the method of numerical simulations and created 3D modal.

Chapter five. This chapter discusses the experiments and results that obtained after conducting the mechanical tests, all the experimental results of this study are discussed in detail. The experimental results include, bending test, tensile test, thickness of coatings, and surface roughness measurements. Then compared between result of the real experimental and numerical simulation process.

Chapter six. This chapter recapitulates the conclusions of the present works and recommends the possible future works.

CHAPTER TWO

COATING

2.1 Introduction of Coating

A coating is a covering applied to surface of material, regularly referred to as a substrate. The purpose of apply coating is for decorative, practical, or both of them. Coating itself may be an all-over coating, covering completely the substrate, or it may covers only parts of the substrate material. Practical coatings may be applied to change the surface specification of substrate, such as wettability, corrosion resistance, adhesion, or wear resistance. Coating is a covering which can be applied to surface of object, typically titled as substrate. The aim of coating application is enhancing the value of the substrate by improving its appearance, wear resistance, corrosion resistant property, etc. Process of coating involves applying a thin film of a functional material to a substrate. Functional material may be organic or inorganic; metallic or non-metallic; solid, liquid or gas. This must be sincere conditions of classification of coatings [20].

2.2 Method of Coating

Many different technological methodologies have been operated to coat the surface of sheets metal ensuring uniformity and quality of performance of the polymer coatings. These methods are:-

2.2.1. Coil Coating

Coil coating is one of the regularly used coating techniques in the field of manufacturing. It is an automatic and continuous process, which is capable of coating very large sheets on both top and bottom in one single layer process, as shown in Figure 2.1[1].



Figure 2. 1: Coil coating process [1]

In coil coating process, sheets metals are initially cleaned to provide a clean surface. The second step is to pretreatment the surface by using some kinds of specific chemical materials. In the following step, primer is to be applied on coating surface to provide flexibility and corrosion resistance by corrosion inhibitors exist in the primer. Primer is then cured as the material goes through the remedy oven at carefully and closely regulated temperature [21]. Finally, a top coat is applied on the primer and is yet passing through the oven for curing, as shown in Figure 2.2.

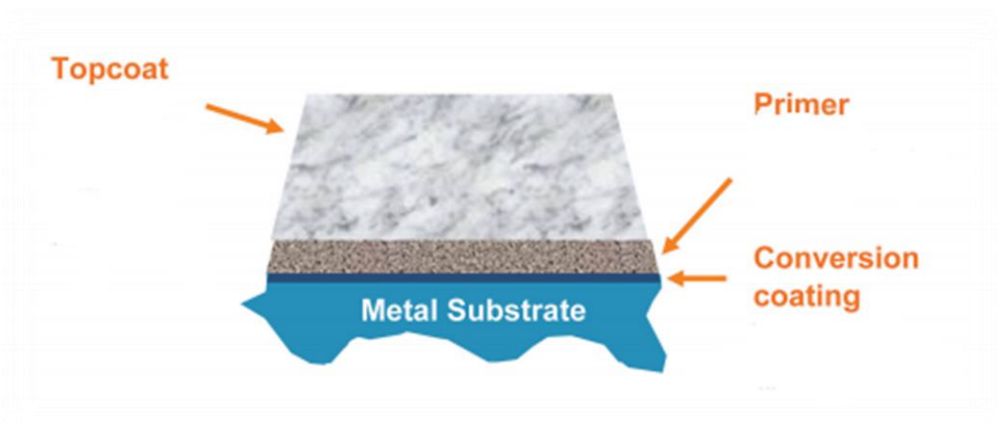


Figure 2. 2: Typical build-up of a coil paint coating [21]

2.2.2. Spin Coating

The spin coating for material is a process of coating a flat surface by a thin liquid film smoothed by a fast rotation of the surface. This process is usually used in semiconductors industry for depositing layers of photoresist above silicon wafers. The photoresist layers are used in photolithographic patterning of integrated circuits. Spin-coater basically a turntable kept under vacuum conditions. To achieve spin coating, a substrate is situated on the turntable and then a liquid is deposited at the center of substrate. This is followed by a fast rotation of the turntable. The liquid is distributed outwards to the edge of the substrate and forms a thin film of a comparatively uniform thickness; Figure 2.3 shows the spin coating [22].

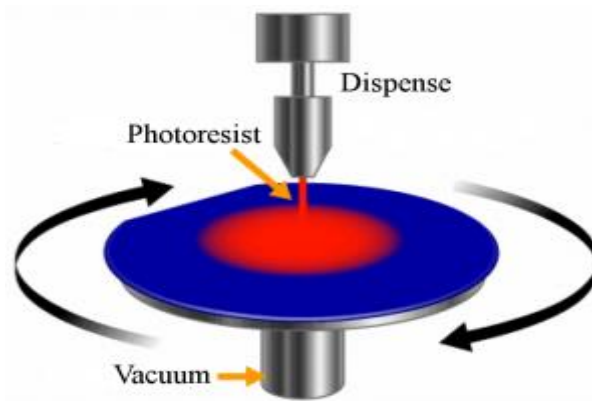


Figure 2. 3: Spin Coating [22]

2.2.3. Physical Vapor Deposition

Physical vapor deposition (PVD) describes a change of vacuum deposition methods which can be used to produce thin films and coatings. PVD is characterized by a process in which the material goes from a condensed phase to a vapor phase and then back to a thin film condensed phase. PVD is used in the construction of items, which require thin films for mechanical, optical, or electronic and chemical functions. Examples include semiconductor devices such as thin film solar panels [23].

2.2.4. Chemical Vapor Deposition

Chemical vapor deposition (CVD) is a chemical process used to produce high quality, high-performance, solid materials. The process is regularly used in the semiconductor industry

to produce thin films. In classic CVD, the wafer (substrate) is exposed to one or more volatile precursors, which react and/or decompose on the substrate surface to produce the desired deposit. Micro fabrication processes widely use CVD to deposit materials in various forms; these are mostly used to obtain very thin and accurate coating thickness. CVD is extremely useful in the process of atomic layer deposition at depositing extremely thin layers of material [24].

2.3 Polymer and Polymer Properties

Polymers are found everywhere. Polymers exhibit confluent bonding within chains and secondary bonding (Vander Walls bonding) between each layer and there are three major types [thermoplastics, thermosets, and elastomers]. Polymers as (Epoxy, polyester, polyvinyl ester, phenolic resin, polystyrene, polyurethane resin, natural rubber, silicone rubber, etc.) are low weight, stiffness, corrosion resistant materials with low strength and they are not suitable for use at high temperature [25]. These polymers are, however, relatively expensive and are readily formed into a variation of shapes. Engineering polymers are designed to give better performance or improved strength at elevated temperatures. Polymers are used as engineering materials in the neat form, or in combination with a large diversity of additives, both organic and inorganic. These additives may be, among others, plasticizers which reduce the rigidity or brittleness of the material, fillers which increase the strength and load deflection behavior under load, or stabilizers which protect the polymer against ultraviolet radiation. They are thermally and electrically insulated. Polymers have low density and high resistance to chemical reactions [26].

Mechanical properties of the polymers are sensitive to temperature and the strain rate, on increasing the temperature and decreasing the strain rate, the material becomes softer and ductile. These advantages and properties of polymers make them a perfect choice to be used as a coating on metal sheets. Polymer coatings are used in many applications, such as for car components, building roofs, beverage cans, packing materials, etc [27].

Many additives are added to improve the properties of polymers. Wax is added to improve lubrication, and ceramic rollers, natural rubber, Nano powders, and Nano fibers to improve the mechanical properties. The new material is defined as the composites materials, are made by combining two or more materials embedded in another material called matrix often once that

have very different properties. The two materials work together to give the composite unique properties. The reinforcing material can be metal, ceramic or polymer.

In this study, the matrix is commonly referred to the phase that is continuous and surrounds the dispersed phase (epoxy - fly ash) composite is a two-phase composite where epoxy is the matrix and fly ash particles constitute the dispersed phase.

2.3.1 Epoxy Resin

One of the most common of polymers materials is the epoxy resin which has been widely used as protection system of heterogeneous composites in many structures, because of its outstanding procedure ability, excellent thermal resistance, good electrical insulating properties, strong adhesion, and affinity to heterogeneous material with a higher mechanical property under heavier loading. They have a wide range of physical properties, mechanical capabilities and processing conditions that make them invaluable compared to other thermosetting resins [28].

Epoxy resin systems are increasingly used as matrices in composite materials for a wide range of automotive and aerospace applications, and for shipbuilding or electronic devices. They serve as casting resins, adhesives, and as high performance coatings for tribological applications, however, because the polymer matrix must withstand high mechanical and tribological loads, it is usually reinforced with Nano fillers. As a laminating resin, their increased adhesive properties and resistance to water degradation make these resins ideal for use in applications such as boat building. They also have good adhesion to other materials, good environmental resistance, good chemical properties and good insulating properties [29]. Many type of epoxy are available and the general mechanical characteristics of epoxy resin are shown in Table 2.1.

Table 2. 1: General mechanical characteristic of epoxy resin [30]

Tensile modulus	3-5 GPa
Density	1.100-1.500 Kg/m ³
Tensile strength	60-80 MPa
Tensile elongation	2-5 %
Flexural strength	100-150 MPa
Heat deflection temperature	290 °C
Shear strength	30-50 MPa

2.3.2 Fly Ash Reinforcing Material

Fly ash powder is a mixture of ceramics oxide; it can be applied as a strengthening material for reinforcing polymer matrix composites. It improves the mechanical and physical properties of the polymer composites [31]. Fly ash powder is a byproduct ceramic powder of generator of coal combustion in generation stations of electric power. It is composed of soft ball-shaped particles either hollow or solid, and be either of a crystalline or amorphous structure (random) [32].

The major ingredients of the fly ash include: silicon oxide (SiO₂), aluminum oxide (Al₂O₃) and iron oxide (Fe₂O₃) furthermore, secondary ingredients which include: (TiO₂, SO₃, Na₂O, K₂O and MgO) and each kind of fly ash has different chemical composition depending on the source of coal burning [33]. Fly ash colors range from black to gray to dark brown based on the mineral and chemical ingredients of coal burning as shown in Figure (2.4). The fly ash powder is obtainable in large amounts from generating stations of electric power and for this reason; it can be easily obtained at low cost. The generally important characteristics of fly ash include: hardness and high toughness and high electrical strength. The physical characteristics of fly ash powder depending on the type of burning coal and conditions of combustion [34].

The physical characteristics of fly ash powder depending on the type of burning coal and conditions of combustion. Table 2.3 illustrates the generally important physical characteristics of the fly ash powder according to the international standard specification (ASTM C618) [35], and the chemical composition of fly ash is fully depends on the chemical composition of the burned coal which produces it [36].

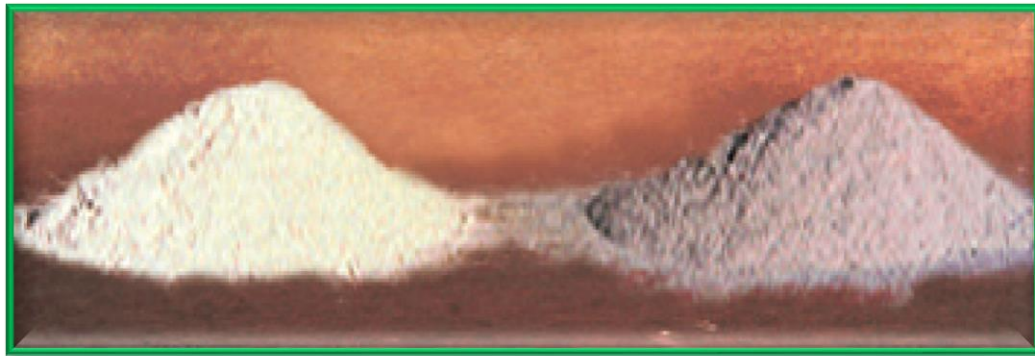


Figure 2. 4: Variation in the colors of fly ash

Table 2. 2: Physical properties of the fly ash [35]

Physical properties	Description
Color	Black to gray to brown
Specific gravity	1.3-4.8
Density	1.9-2.8 gm/cm ³
Melting point	1200-1400 °C
Specific surface area	250-600 m ² /Kg
Particle size	1-100 μm

2.4 Forming of Sheet Metal

The sheet metals forming process consists of cutting operations or operations, there is many types of forming some of these processes as bending, stretch forming and deep drawing, are examples of a plastic deformation process. This procedure involves a change in the shape of work-piece (as desired) without any cutting operation. Performance of the process depends

on properties of sheet metal, coating material and forming conditions. The bending procedure can be found in most assembling industries because of its edibility [37].

2.4.1 Bending

Bending of sheet metal is a common and pivotal process in manufacturing industry, and it is the plastic deformation of the work over an axis. Similar to other metal forming processes, bending changes the shape of the work piece, while the volume of material will remain the same. The use of bending is determining the mechanical properties. In bending, a uniform sheet is linearly strained along an axis lying in the neutral plane and perpendicular to the length of the sheet. Different bending operations are V-bending, U-bending, roll bending, edge bending etc. If a v shaped die and punch are used, the bending is called v-bending. If the sheet is bent on the edge using a wiping die, it is called edge bending. Also, air bending is the bending of sheets easily between an upper roll or punch and a lower die freely. In roll bending, a pair of rolls supports the plate to be bent and the upper roll applies the bend force as shown some types of bending in Figure 2.5 [38].

Smooth rectangular samples without notches are generally used for bend testing under three-point or four-point bend arrangements; three-point bending is capable of 180° bend angle for welded materials. Considering a three- point bend test of an elastic material, when the load P is applied at the midspan of specimen in an x-y plane, stress distribution across the sample width is demonstrated in the stress is essentially zero at the neutral axis N-N. Stresses in the y axis in the positive direction represent the tensile stresses whereas stresses in the negative direction represent the compressive stresses as shown in Figure 2.6 [39].

Within the elastic range, brittle materials show a linear relationship of load and deflection where yielding occurs on a thin layer of the specimen surface at the midspan. This in turn leads to crack initiation which finally proceeds to sample failure. Ductile materials however provide load-deflection curves which deviate from a linear relationship before failure takes place as opposed to those of brittle materials previously mentioned also difficult to determine the beginning of yielding in this situation.

Therefore, it can be seen that bend testing is not suitable for ductile materials due to difficulties in determining the yield point of the materials under bending and the obtained stress-strain curve in the elastic region may not be linear. As a result, the bend test is therefore more

appropriate for testing of brittle materials whose stress-strain curves show its linear elastic behavior just before the materials fail [40].

The flexural strength, or modulus of rupture, describes the material's strength:

$$\text{Flexural strength for three - point bend test} = \sigma_{\text{bend}} = 3FL/2wh^2 \quad (2.1)$$

Where F is the fracture load, L is the distance between the two supported points, h is the Thickness of the specimen and W is the width of the specimen.

End test are similar to the stress-strain curves; however, the stress is plotted versus deflection rather than versus strain, or the flexural modulus (E_f), is calculated in the elastic region.

$$\text{Flexural modulus} = E_f = fl^3/4\delta \quad 3h^3 \quad (2.2)$$

Where δ is the deflection of the beam when a force F is applied.

The distribution of shear stress is parabolic, with a maximum of the neutral axis and zero at the outer surface of the beam, the maximum value is given by equation (2.3):

$$\text{Maximum shear stress } \tau = 3f/4wh \quad (2.3)$$

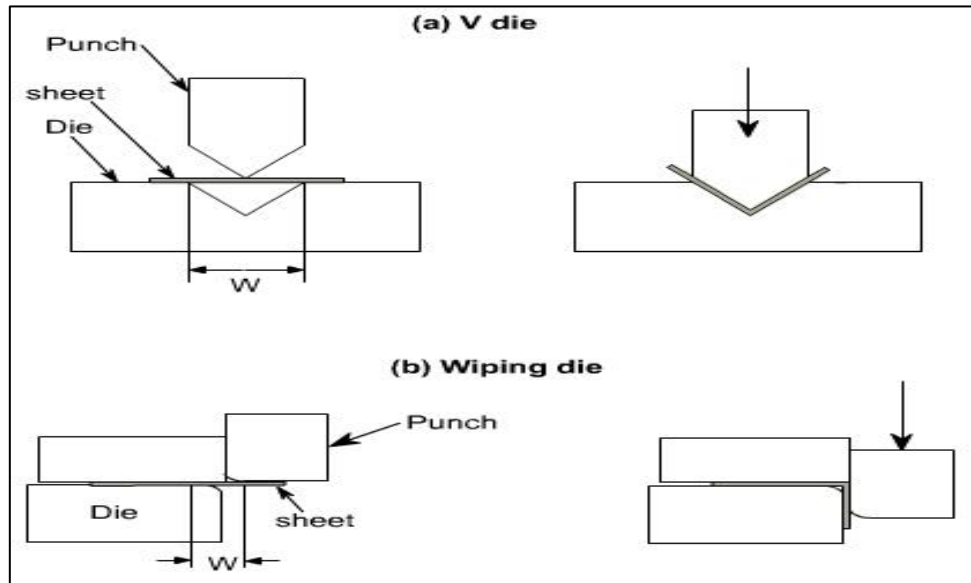


Figure 2. 5: Some of bending types [39]

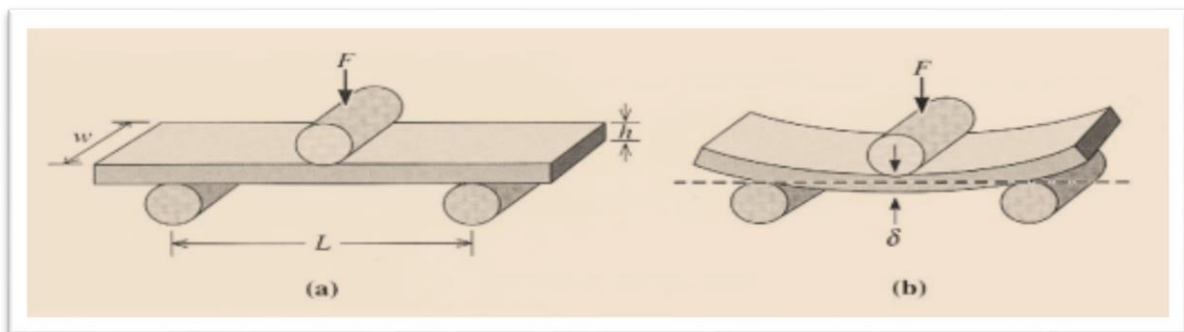


Figure 2. 6: Testing of a rectangular bar under a) three-point bend b) The deflection obtained by bending [40]

2.5 Defects in Coatings during Forming

During forming, coating has to be free from defects, like scratches, cracks, chipping and peeling. Thus, it is important to know the types of defects and causes for defects. Surface wear and delamination are the two major defects observed, as shown in Figure 2.7, the material is removed from the surface of the coat when in contact with sharp edges or corners. This forms scratches or damages on the surface, leading to surface damage of polymer coatings.

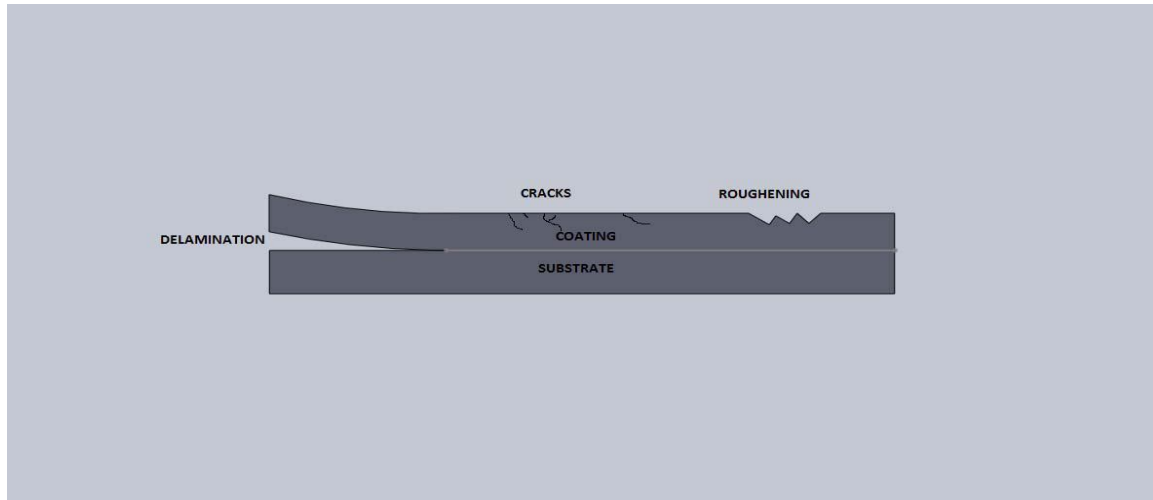


Figure 2. 7: Deficiencies in Coating [41]

Deprived adhesion and discontinuity between top coat and the substrate leads to delamination. These defects cause loss of the attractive and protective properties of the product and should be prevented. [41]

2.6 Surface Damage during Forming

Surface damage of the polymer coating can be observed during forming of coated sheet metal. Damage in the form of scratches and loss of glossiness on the surface of the coatings is seen. The suitable control of parameters during forming and detailed treatise of the surface wear can reduce the surface damage of coatings [42].

2.6.1 Surface Wear

Wear of surface is defined as a gradual injury of material from the surface of one body due to sliding interaction with another body. In sheet metal forming, surface wear takes place by different mechanisms leaving behind scratches on the surface of final product. According to Schuler, wear can be classified into five basic ways [43]. They are deformation, adhesion wear, and abrasive wear, wear at surface layer and fatigue wear. Wear is shown in Figure 2.8 revealing

that the mechanisms have different depth effects on the material. Wear at surface layer is also called as tribo-chemical wear mechanism. Due to thermal and mechanical processes occurring at the interface, it forms an interfacial layer between the sliding pair in the form of oxide or reaction layers. These layers have both positive and negative effects. The shear strength of these layers is much smaller than that of the bulk metal, therefore it deforms easily under frictional stress. However, it acts as a protective layer for the substrate underneath under small loading [44].

Adhesive wear is caused by adhesion of the material to the counter face under sliding. Throughout a forming process, the plastic deformation occurs at the asperities causing the lower hardness material to weld to the counter face having higher hardness value. Selecting the sliding pair having different chemical compositions and similar mechanical properties reduce the adhesive wear. It can also be minimized by better surface finish and use of lubricants, the lowest wear is manifested in the case of metallic and non-metallic counter faces with similar hardness. Non-metallic coatings on metal substrate show a high resistance to adhesive wear and corrosive wear [45].

Thin polymer coatings are generally applied on the metal substrates to reduce the galling tendency when sliding against metal counter face. Abrasive wear is caused by harder irregularities causing cutting or ploughing on the softer counterpart. This wear results in scratches on softer surface. This is generally seen as a secondary wear mechanism occurring after adhesive wear where the adhesive particles sticking to on the surface abrades the counter face. Ploughing component of friction is responsible for abrasion wear. Abrasion wear reckons on the relative hardness of frictional pair in play. Fatigue wear causes surface failure due to repetitive stress from the hard irregularities on the counterpart. It is generally seen as a long term wear. Surface wear in metal forming is related to friction conditions during the process, very high coefficient of friction (COF) will lead to wear on the surface of the sheet which is undesirable and friction is responsible for the stress-strain distribution in the material during the forming process. Thus, study of friction at the interface of die and sheet metal during forming will give a better understanding of surface behavior [46, 47].

CHAPTER THREE

EXPERIMENTAL WORK

3.1 Experimental part

In this chapter, a particular description of the experimental procedure is presented, which includes materials selection, sample preparation methods and the reference of how to prepare molds , how to prepare specimens for each test, methods of testing and detailed description of test instruments used as well as specimens pictures before and after the examination. The following chart (3.1) shows the stages that have been taken in research and diagrams of the geometric shapes required of these samples and for each experiment according to the international standard.

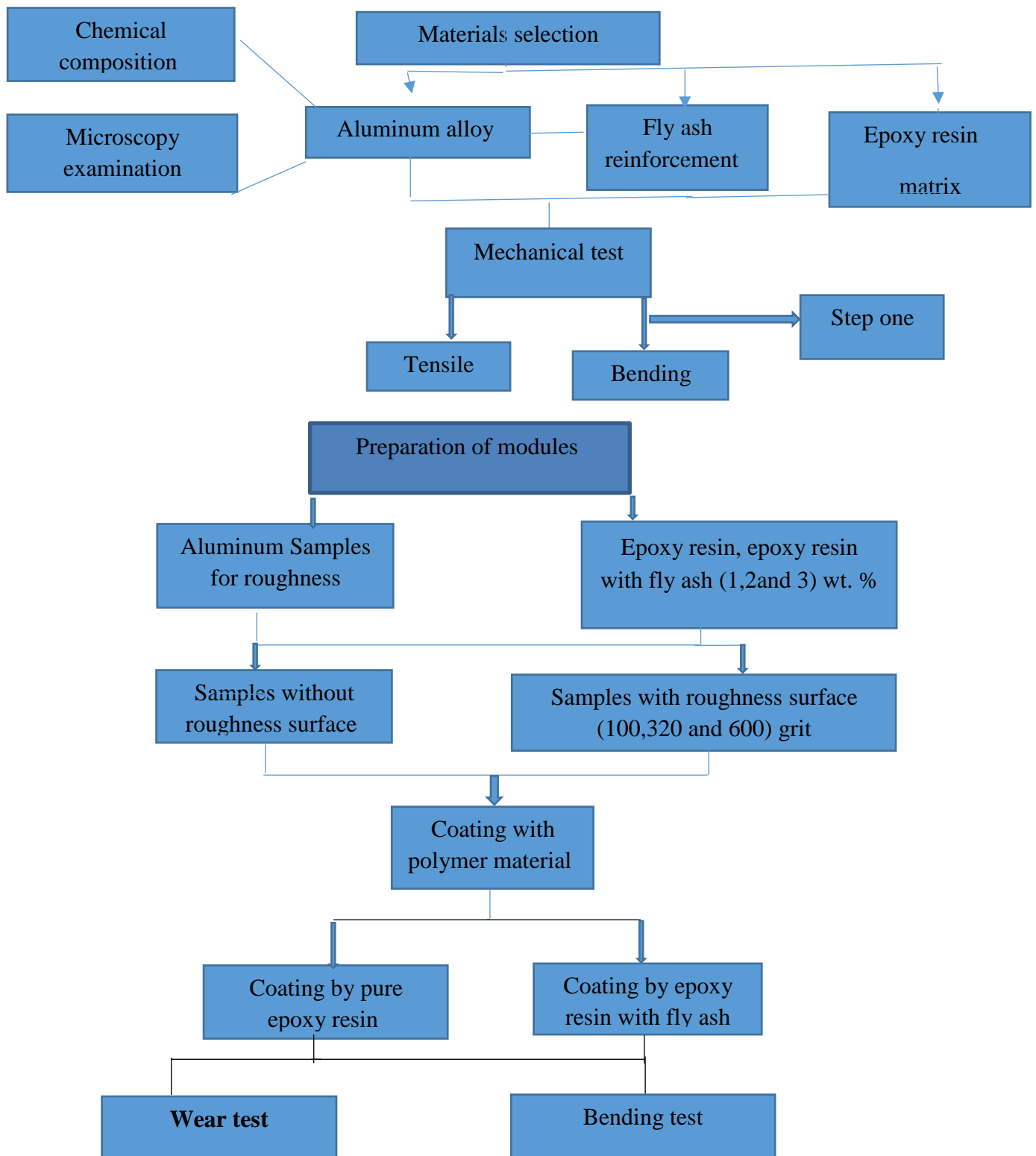


Figure 3. 1: Flow chart of experimental work steps

3.2 The Used Material

In the present work, three different materials were used, these materials are: Aluminum alloy, fly ash and Epoxy resin.

3.2.1 Epoxy Resin

They are a family of thermoset plastic materials which do not divorce reaction produces when they treatment. Epoxy resin for a trademark (Euxit 50 KI) is a liquid of depressed viscosity resin as compared with last thermosets and it is converted to a solid state by addition a hardener (Euxit 50 KII) within a ratio of (1:3) as shown in Figure 3.2 which were provided by Egyptian Swiss chemical Industries Company. The merits of epoxy resin used in this work are given shown in Table 3.1 according to the feature of Product Company.



Figure 3. 2: Epoxy resin and hardener

Table 3. 1: Characteristic of epoxy used in this work according to the properties of Product Company which depended on the ASTM

Tensile strength(MPa)	Compression strength (MPa)	Modulus of elasticity (MPa)
27	70	2800

3.2.2 Fly Ash

Fly ash particles were collected from the atelier as shown in Figure 3.3, in Ceramic Section, and grounded for 15min with the help of agitation motor to form a well powder. Then, this fly ash was saved in a drier at 80°C for 24 hours to eliminate the moisture present in it. After 24 hr., the fly ash was taken out from the drier. Then, the amount of fly ash, epoxy resin and hardener was calculated for three changed composites ratios. Spectrometer inspection was performed on the selected alloy in order to give certainty to the elements content and secure the full chemical structure of fly ash powder. Table 3.2 gives the results of this inspection of the fly ash and Figure 3.4 shown Spectrometer devise.



Figure 3. 3: Fly ash powder

Table 3. 2: The chemical composition analysis of fly ash Nanoparticles

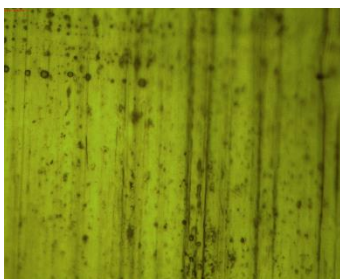
Element Oxide	SiO ₂	Al ₂ O ₃	TiO ₂	MgO	K ₂ O	CaO	Fe ₂ O ₃	Mn ₂ O ₃	Na ₂ O	P ₂ O ₃	L.O.I
The weight (%)	58.2	27.7	1.4	0.05	3.59	0.84	4.99	0.31	0.74	0.34	1.84



Figure 3. 4: Spectrometer device

3.2.3 Aluminum Alloys

Aluminum alloy sheet metal was taken from local markets, made according to the (ASTM) standard with dimension (1m^2) and thickness (0.7 mm) and then was cut off into small pieces. Preparation of sample for inspection was done for cutting, then cleaning and polishing. Spectrometer inspection has been complete on the selected alloy in order to give certainty to the elements content and secure the full chemical composition of the alloy. Table 3.3 gives the results of this inspection of the alloy, the microstructures of the aluminum is shown in Figure 3.5, and the microstructure of aluminum alloy was examined by an optical microscope show in Figure 3.6.



a)



b)

Figure 3. 5: Microstructures to the aluminum at 100 x magnification b) sample of aluminum alloy



Figure 3. 6: Optical Microscope

Table 3. 3: Chemical composition of Aluminum alloy

Element	AL	Mg	Si	P	S	Ti	V
Wt %	92.62	<0.012	0.0649	<0.00038	<0.002	0.123	<0.00047
Element	Fe	Co	Ni	Cu	Zn	As	Zr
Wt %	5.047	0.228	0.121	0.0068	0.2358	0.00009	<0.050
Element	Ag	Cd	Sn	Sb	W	Pb	Mn
Wt %	0.0157	<0.00045	<0.00032	0.00094	0.00089	0.0106	0.115
Element	Cr	Mo	Nb				
Wt %	<0.001	0.359	0.0085				

3.3 Procedure

3.3.1 Samples Preparation

Specimens preparation involves several points starting from the aluminum alloy selection, mold preparation and completed with the samples cutting.

3.3.2 Surface preparation

Surface preparation is the essential step for coating purpose, and as the first step treatment of a substrate before the application of any coating, aluminum alloy was prepared by cutting the sheet metal into samples according to inspection used and then cleaning by using washing powder to remove the outer oxide layer. Then, the samples were first washed by water, equalized the acid with sodium hydroxide (NaOH) and then washed with water again. The work surface of samples was abraded with silicon carbide abrasive paper down from (100 grit, 320 grit and 600 grit), then they were rinsed with alcohol, dried in hot air, and then, the coating was directly done to avoid the samples from oxidation, which encourages the failure of coats.

3.3.3 Roughness of the surface

This test was accomplished for [12] samples of aluminum alloy] to measure the surface roughness after treatment with different grits, [(4) Samples with 100 grit, (4) Samples with 320 grit and (4) Specimens with 600 grit]. The measurement was done by fixing the sample on the device surface, and applying the probe of the device perpendicular to the sample for 32 second and taking the readings on different spaces [Five reading for each sample] on the surface of sample, as shown in Figure 3.7. Figure 3.8 expressions the samples of surface roughness test, and Table 3.4 lists the roughness values for samples in μm units.

Table 3. 4: Surface roughens values in μm units

	1	2	3	4	5	Average
100 grit	2.000	1.690	1.603	1.700	1.600	1.718
320 grit	0.820	0.933	0.973	0.850	1.000	0.915
600 grit	0.540	0.600	0.553	0.460	0.546	0.534



Figure 3. 7: Roughness surface device



Figure 3. 8: Samples of roughness surface test

3.3.4 Coating Process

3.3.4.1 Coating by Epoxy Resin

The coating process was done after the surface roughness process. Hand lay-up is the simplest method and a flexible method that allows the user to optimize the part by placing different types of material. The first stage is coating by epoxy resin alone, as presented in Figure 3.9, in as follows:

- Aluminum sample without roughness (one sample).
- Aluminum samples with roughness (100 grit, 320 grit, 600 grit) [three samples].

Preparation of pure epoxy: The epoxy and hardener must be mixed slowly by a glass rod to thwart bubbles that may be produced, and this process was achieved at the ambient conditions.

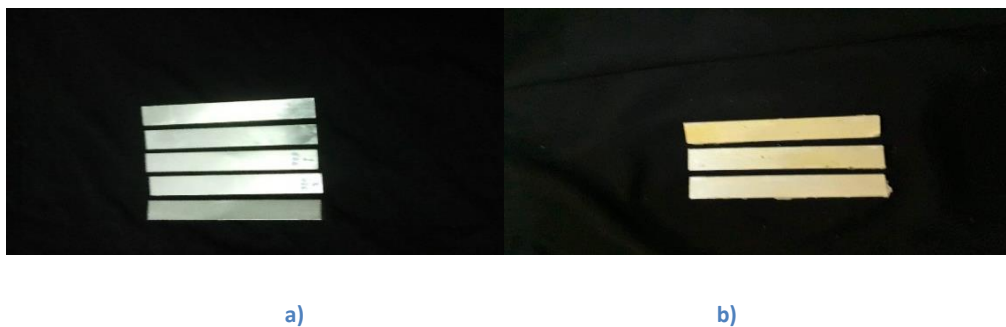


Figure 3. 9: Some of aluminum alloy samples, a) before coating b) after coating

Other samples were coated by epoxy resin mixed with fly ash.

3.3.4.2 Coating by Epoxy resin with Fly ash

The steps of epoxy resin with fly ash coating were done as following:

1. Weighing of epoxy resin according to mold size, and the weight of fly ash was premeditated according to the required weight fraction (1, 2, and 3) wt. % of epoxy resin and weighed of fly ash by using an electronic balance with accuracy (0.0001) as shown in Figure 3.10. Table 3.5 shows the epoxy resin with different fly ash powder ratios after the mixing process is continued to obtain a completely homogeneous mixture.

Table 3. 5: Epoxy resin with fly ash ratios

EP:FL	100:0	99:1	98:2	97:3
-------	-------	------	------	------

2. Manual mixing the Fly ash with epoxy resin for nearly 10 minute at room temperature continuously and slowly to elude bubbling formation during mixing until a homogeneous case of the mixture and then adding hardener to the mixture with a gentle blending as shown in Figure 3.11.
3. Placing the samples in a mold, and then the mixture (epoxy resin with different fly ash ratio) was poured into the mold to cover the aluminum samples. The mixture was poured from one angle into the mold (to avoid bubble formation which reasons cast damage) and the uniform pouring was continued till the mold was filled to the required grade.



Figure 3. 10: Electronic balance

4. After curing the polymer coated samples for 24 hr. at room temperature (27°C), all the polymer coated samples were then hereafter cured in an electrical oven at 55° C aimed at 1 hr. This step is imperative to achieve a comprehensive polymerization, best

coherency, and to relieve the backward stresses. Figure 3.12 depicts the specimens before and after coating.

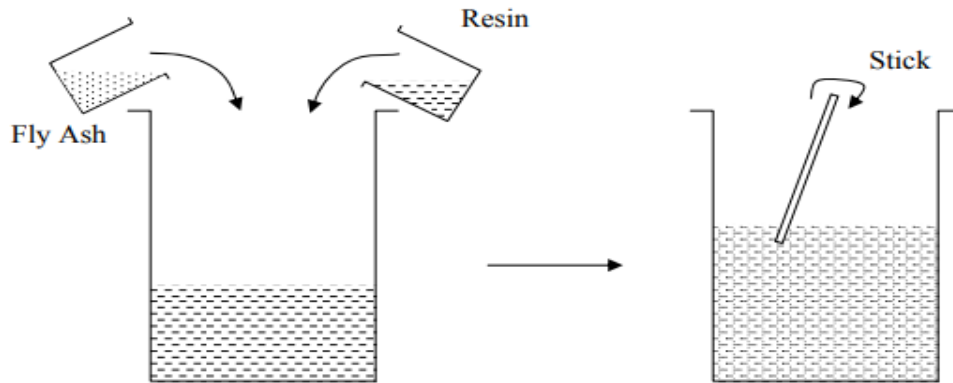


Figure 3. 11: The method of mixing the epoxy with fly ash



A)



B)

Figure 3. 12: Aluminum alloy specimens a) before coating b) after coating

3.4 Mechanical Test

3.4.1 Tensile Test

3.4.1.1. Tensile Test of Aluminum Alloy

Tensile testing will be performed to define tensile properties. In tensile testing, a sample is located in the grips of movable and stationary fixtures in a screw driver device, which tow the sample until it breaks and measures applied load versus elongation of the sample. The testing process requires specific grips, load cell, and extensometer for each material and sample type. The extensometer is calibrated to measure the smallest elongations. Output from the device is recorded in a text file including load and elongation data. Elongation is typically measured by the extensometer in volts and must be converted to millimeters. Mechanical properties are determined from a stress vs. strain plot of the load and elongation data.

To determine the material properties of the aluminum sheet, specimens were and tested according to ASTM standard E8M specification, the specimens were first prepared by cutting machine and then loaded until fracture occurred. Three specimens were tested for the test condition to check the repeatability of the results as shown in Figure 3.13, and Figure 3.14 displays the tensile test standard specimen. The tensile tests were applied and conducted under a constant cross head speed 1 mm / min using a WDW- 200E Computer Controlled Electronic Universal Testing Machine, Figure 3.15.

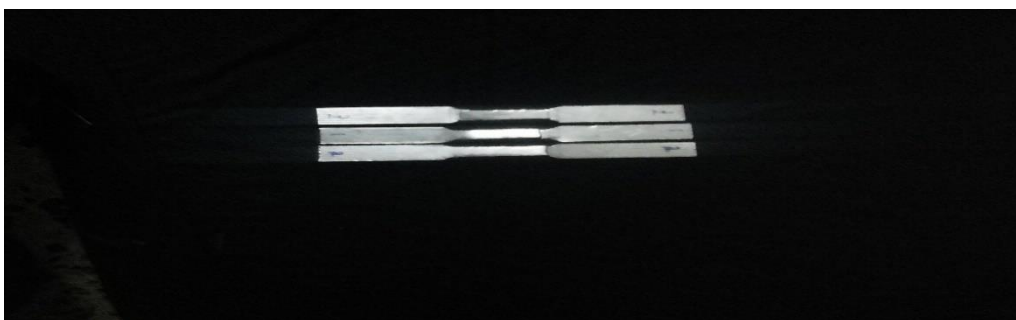


Figure 3. 13: Samples of tensile test

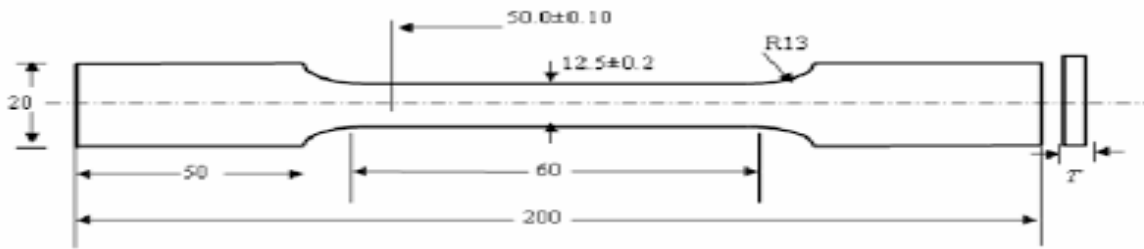


Figure 3. 14: Tensile test standard specimen



Figure 3. 15: Experimental specimens test

3.4.1.2 Tensile Test of Epoxy Resin

The casts of specimens used in tensile test were fabricated from stainless steel. The internal base and inside walls of the mold were covered with a tender layer of release agent to avoid the spearing between the cast matter and the mold partition. One sample was set for tensile test apparent in the Figure 3.16, the tensile properties (tensile strength, modulus of elasticity) were obtained agreeing to ASTM D638M- 87b for samples at 20°C, The tests were passed out using the microcomputer controlled electronic universal mechanical test the machine. The test was performed by using Universal Testing Machine type as shown in Figure 3.15, with capacity load (50 KN) and strain rate of (5 mm/min) at room temperature. Figure 3.17 shows standard specimens for testing.



Figure 3. 16: Sample of tensile test (epoxy resin)

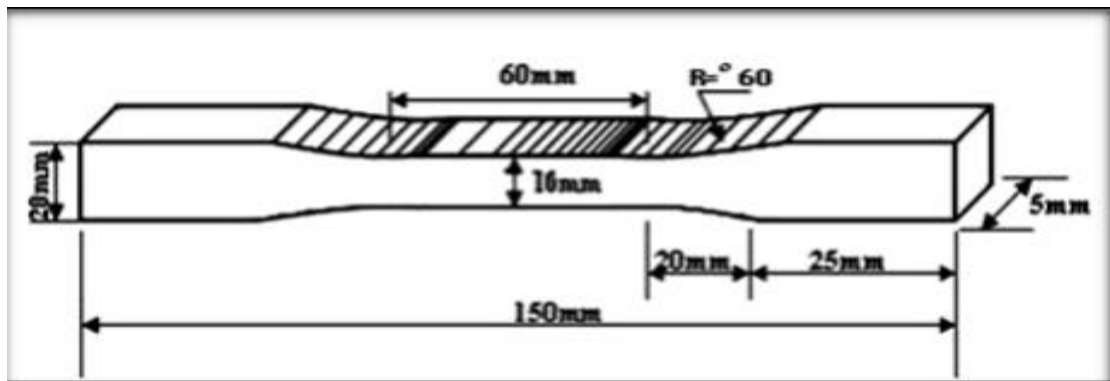


Figure 3. 17: Tensile test standard specimen

3.4.1.3 Tensile test of Epoxy Resin with different ratios of fly ash

Tensile testing is a destructive characterization technique. The (American Society for Testing and Materials) provides the following relevant standard test method (ASTM D638) is one of the most common material strength specifications and covers the tensile properties of unreinforced and reinforced material. To get the proper dispersal of epoxy and fly ash powder mechanical stirring was done at 2000 rpm for 2 hours, fly ash of 1 wt. %, 2 wt. % and 3 wt. % were added to the epoxy resin and stirred for 2 hours. To reduce the viscosity of epoxy solution preheating at 60°C for 30 min. After that the sol was mixed with the hardener in the relation of 1:3 by weight, and then mixing, mechanical stirring up to 15 minutes was done, so the mixture molded in tensile mold, the molds of specimens used in tensile test were made-up from stainless steel. It is kept in electric oven (1 hour) at 50 C⁰ after that placing in air 24 hours. The tensile test was completed with a test rapidity of 5 mm/min.

3.4.2. Bending Test

3.4.2.1 Bending test of aluminum alloy samples coated

Bending behavior of the prepared sample was studied using a three - point test implement, the test was done at room temperature and after fixing the ends of the sample on the supports of the mechanism, the weights were increased gradually on the hanger at the middle of the sample. From the reading of the dial gauge, the deflection of the samples were determined until the ultimate deformation, and from these data a curve of load deflection was produced and bending modulus can be calculated . Samples of dimensions (120×20×0.7) (L×W×T) mm were prepared according to the standard measurements as shown in Figure 3.18 and using microcomputer controlled electronic universal automatic testing machine with a velocity rate of about (10 mm/min), as shown in Figure 3.19.

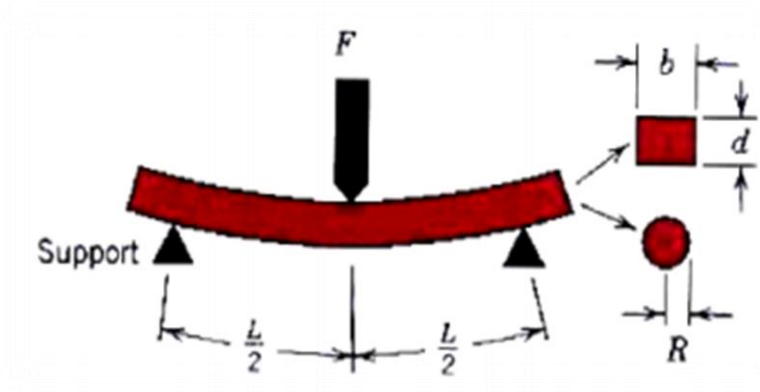


Figure 3. 18: Three- point bending test (simple specimen)



Figure 3. 19: Specimens after bending



Figure 3. 20: Bending machine

3.3.4.2 Bending test of Epoxy resin

Flexural test is done according to (ASTM D790) at room temperature using microcomputer controlled electronic universal mechanical test machine with a speed rate of about (5 mm/min) as shown in Figure 3.20 and Figure 3.21 showed the case of epoxy resin.

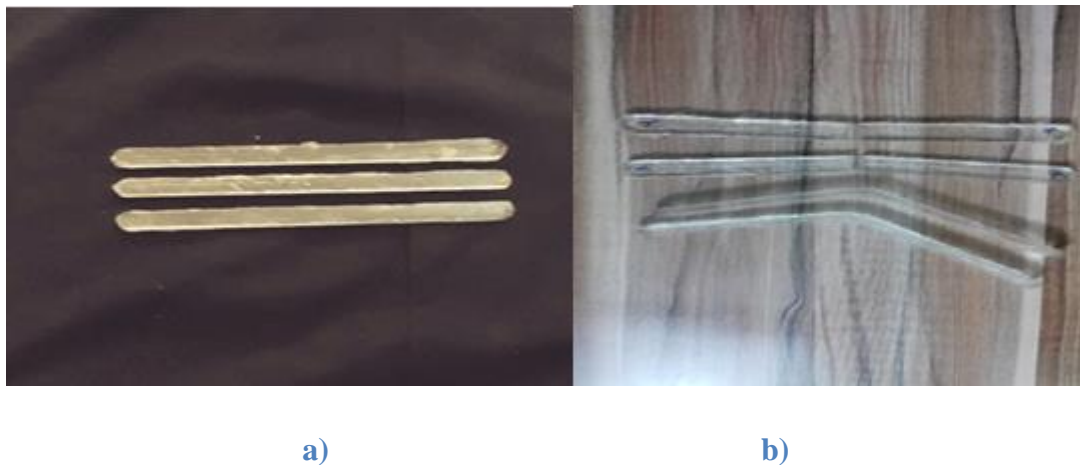


Figure 3. 21: Samples of epoxy resin a) before testing b) next testing

3.4.3 Wear Test

This test was done by preparing selection sample at room temperature and weigh the it before test with a delicate balance after that show the disk in place of the ad hoc working to clean it by smoothing paper before the start of experiment, fixing weight is required and which is perpendicular to the sample after install it in the place. Reset stopwatch and occupy the device with operate a stopwatch as well as in that one after (5 min) of the device stopped operating, finally open the test sample from the device and weigh the sample in the delicate balance and record weigh ,Figure 3. 22 show the wear test device.



Figure 3. 22: Wear test device

CHPTTER FOUR

NUMERICAL SIMULATIONS

4.1 Interdiction

Numerical simulations are used to evaluate the mathematical model of a process and estimate its characteristics. It is an easy and efficient way to solve and provide approximate solutions to a problem. The present work aims at simulating the experiment using numerical method and comparing the results to get a better understanding of the problem. These simulations were further used to change the variables independently and predict the results just by performing numerical simulations (without running experiments). The finite element (FE) method, a powerful numerical technique, has been applied in the previous years to a wide range of engineering problems. Although much FE analysis is used to validate the structural integrity of designs, additional recently FE has been used to model fabrication processes. When modeling fabrication processes that include deformation, such as sheet metal forming (SMF), the deformation process must be evaluated in expressions of stresses and strain states in the body under deformation including contact issues. The major advantage of this manner is its applicability to a wide class of boundary value problems with little restriction on the work piece geometry [48]. The flowchart of the analysis procedure by using ANSYS package (15) to this model is represented in Figure 4.1. The three plain requirements for the successful commercial application of numerical simulation are:

- (1) Simplicity of request.
- (2) Exactness.
- (3) Computing efficacy.

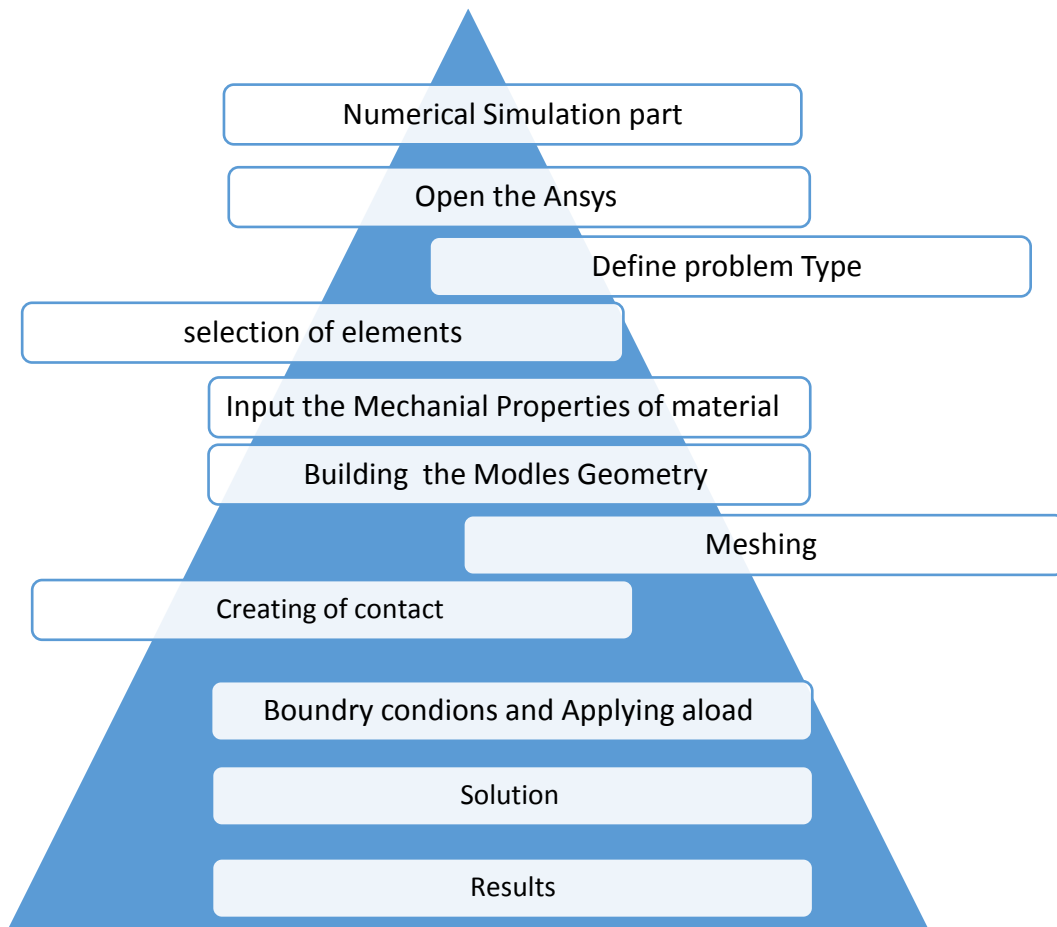


Figure 4. 1: Flow chart of the analysis procedure

4.2 Selections of elements

The ANSYS element bookshop contains more than hundred different portion type [49], the input data for an ANSYS analysis are prepared using preprocessor and the preprocessor (defining the problem) is used to define the element kinds , element real constants , model geometry and material trait .

In the present study the elements hired is solid brick 8 nodes 185 as shown in Figure 4.2, this element is used for 3D modeling of solid buildings and it is defined by 8 nodes having three degrees of freedom at every node translations in the x, y and z direction. It has the mixed construction ability for simulating deformations of almost incompressible elastoplastic

materials and also it has plasticity, hyperelasticity, creep, great deflection, large strain capabilities and stress stiffening.

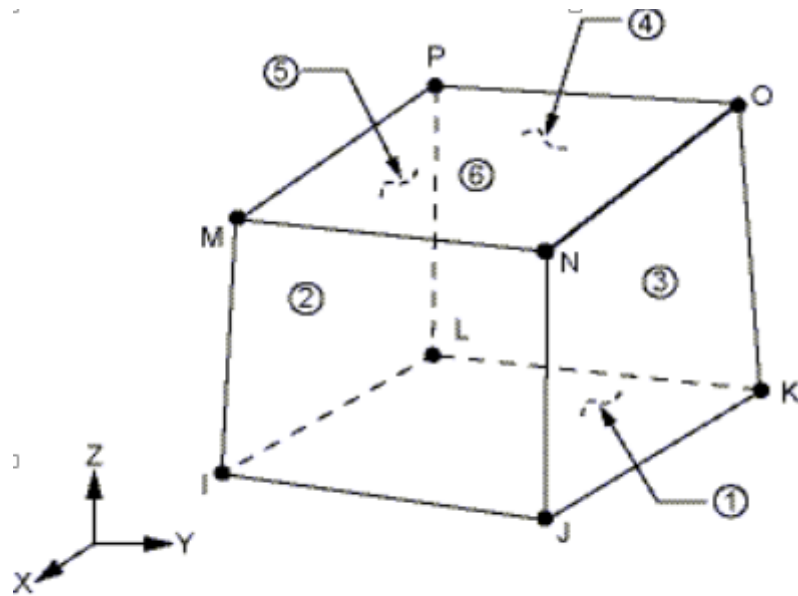


Figure 4. 2: Solid 185 Homogeneous Structural Solid Geometry

4.3 Defining Material Properties

Material advantage is required for most element types. Depending on the application, the set of them may be isotropic, orthotropic, anisotropic, linear, nonlinear, temperature dependent and constant temperature.

In this work, the material is defined by nonlinear and then input properties as the following:

- ❖ Defining the elastic behavior of uniaxial tensile test data from experimental the work for epoxy resin and epoxy with different ratios of fly ash (1, 2 and 3 wt. %.), this property is used to describe the behavior of the materials.
- ❖ The aluminum alloy material is used as a flexible body to build the finite element model.

4.4 Building the Models Geometry

Two types are known for drawing the finite element model in ANSYS: the solid modeling and direct generation. By solid modeling, the geometry of the model is defined, it can be controlled by the size and shape of elements by dividing length of coated sheet metal by (30) division. By means of direct generation, the place of each node and connectivity of each element are manually well-defined. Numerous of convenience processes are available, as delete, add and overlap. The second method is preferred, especially with a complex geometry and was used in the current study, the 3D model is shown in the Figure 4.3 and Figure 4.4 with (20×120×0.7) mm (W×L×T) mm of aluminum alloy samples dimensions and (20×120×0.3) mm (W×L×T) mm of epoxy resin coating layer dimensions, which is a section from aluminum alloy coated by polymer in the experimental work.

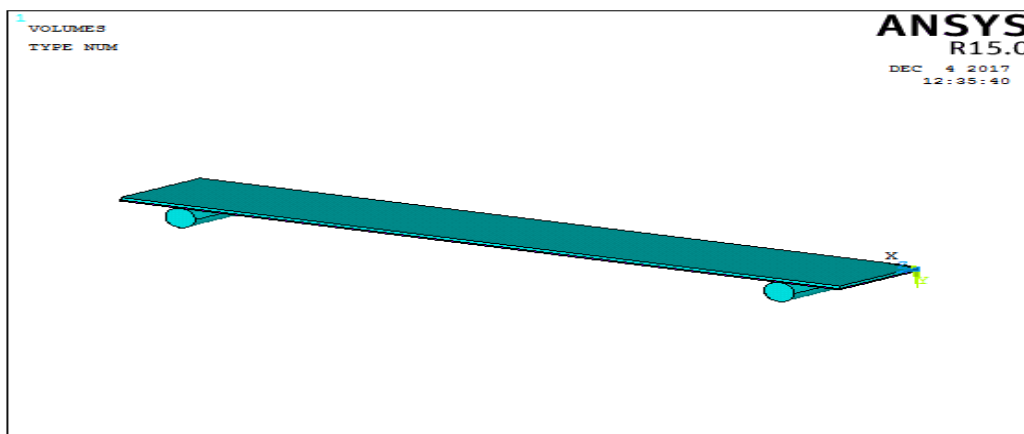


Figure 4. 3: The part in 3D model of aluminum alloy sample

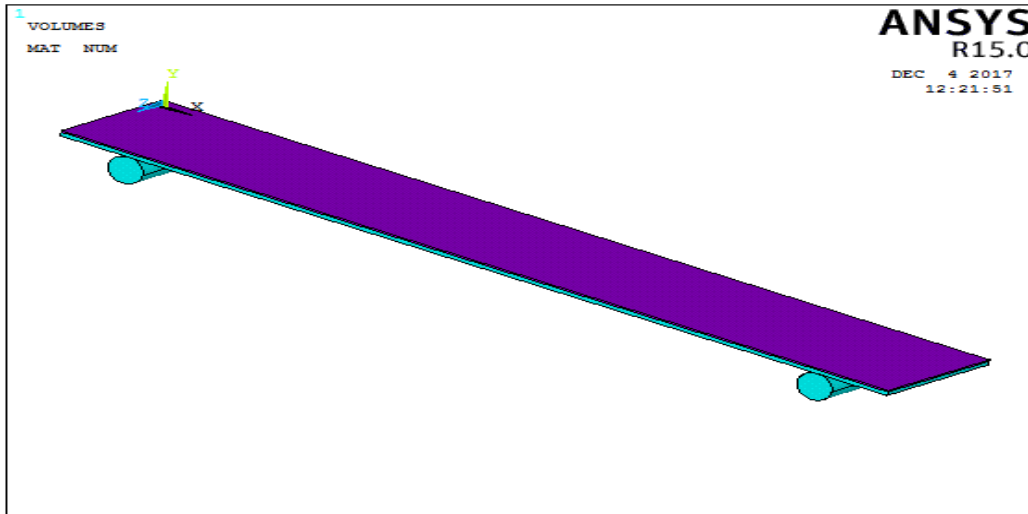


Figure 4. 4: The part in 3D model of aluminum alloy coated by epoxy resin

4.5 Mesh Generation

The meshing stage is an essential step by which the geometric model is transformed into the finite element model. The meshing for a geometrical model is processed by controlling the volume and length of elements, the model after meshing is shown in the Figure 4.5. The geometry of the model is described, and package of ANSYS automatically meshes the geometry with the node and elements. Numerical tests have been done to get the best number of element by using mesh tool and a number of elements used 3D simulation procedure to attain the steady-state solution.

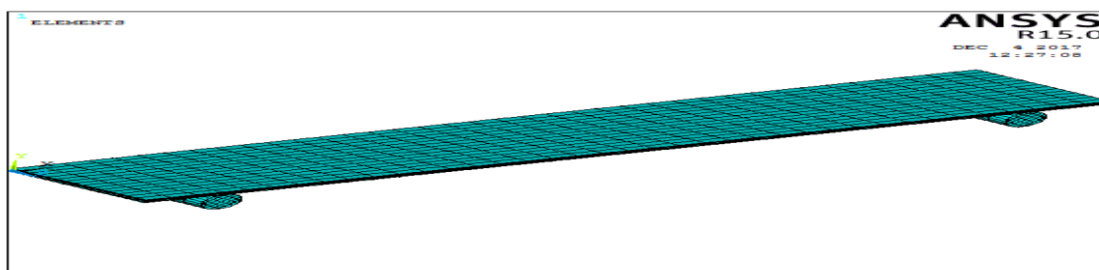


Figure 4. 5: Mesh Generation for Aluminum alloy coated by epoxy resin

4.6 Contact Create

The contacts with the surfaces target comprise the "Contact pair". In present study, the contact pairs are constructed between the aluminum alloy and epoxy resin. A contact pair with a flexible target creates. The types of contact are node to node element, surface to surface and node to surface element. This contact type in this work is surface to surface element, it is well-suited for applications, such as interference fit assembly contact or entry contact, forging and deep drawing problems. These elements are the most broadly used contact elements in ANSYS, due to the many advantages that they are compatible robust, user friendly and feature-rich.

To represent the contact and sliding between the target surface and deformable surface, the CONTA174 is used, as shown in Figure 4.6. This element is suitable for 3D structural and the coupled field contact analyses. The location of element is on the surfaces of 3D solid or the shell elements without mid-side nodes. It has same geometric characteristics like, solid or the shell element which is look that connected with. Contact has occurred when the element surface penetrates one target segment elements TARGE170 on the specific target surface.

TARGE170 were used to represent various 3D (target) surfaces of associated contact element CONTA174, as shown in Figure 4.7. Contact elements themselves overlay the solid, line elements or shell and this describes the boundary of the deformable body and those which are potentially in contact with target surface, defined by TARGE170. This target surface is discretized by a set of target segment elements TARGE170 and paired with its associated contact surface via a shared real constant set.

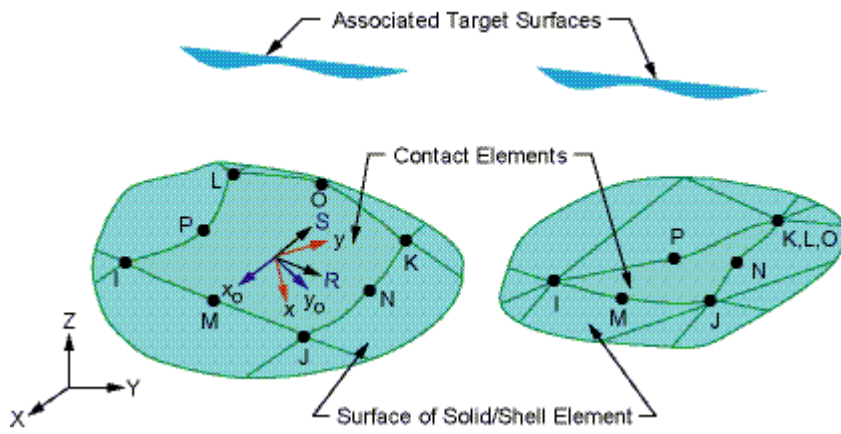


Figure 4. 6: CONTA174 Geometry

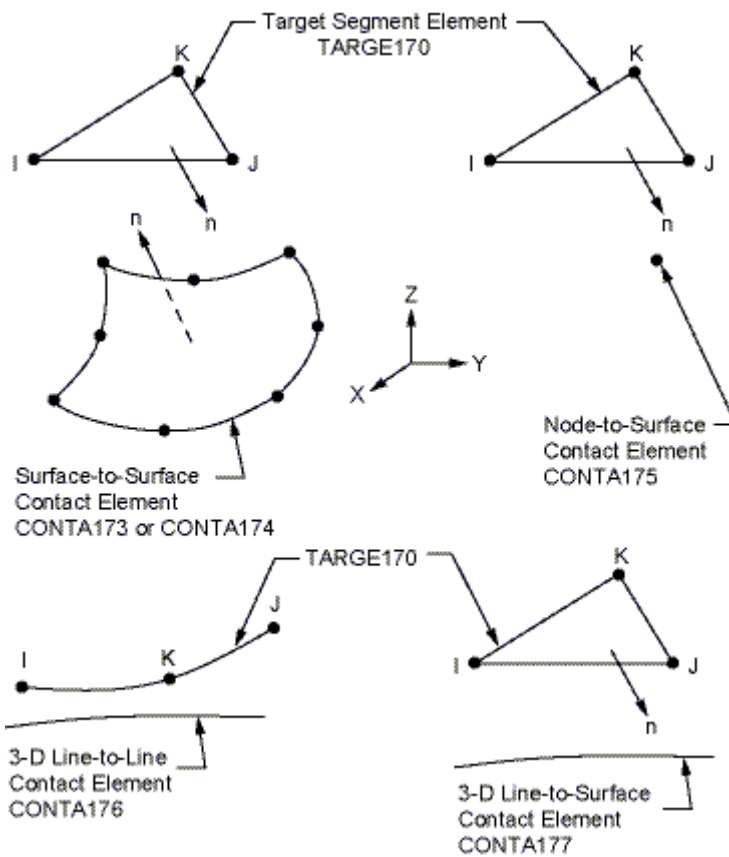


Figure 4. 7: TARGE170 Geometry

4.7 Applying the Load and Boundary Conditions

The load and boundary conditions in this study are applied by using the solution processor with defining boundary condition. This can be defined by applying zero displacement on all degrees of freedom nodes at two side ends and then pointing the load at the mid-span of coated sheet metal which was applied by using the solution processor with load step options .This can be defined by applying a range of force in the positive Y-direction at the nodes in mid- span and then starting the finite element solution, as shown in Figure 4.8.

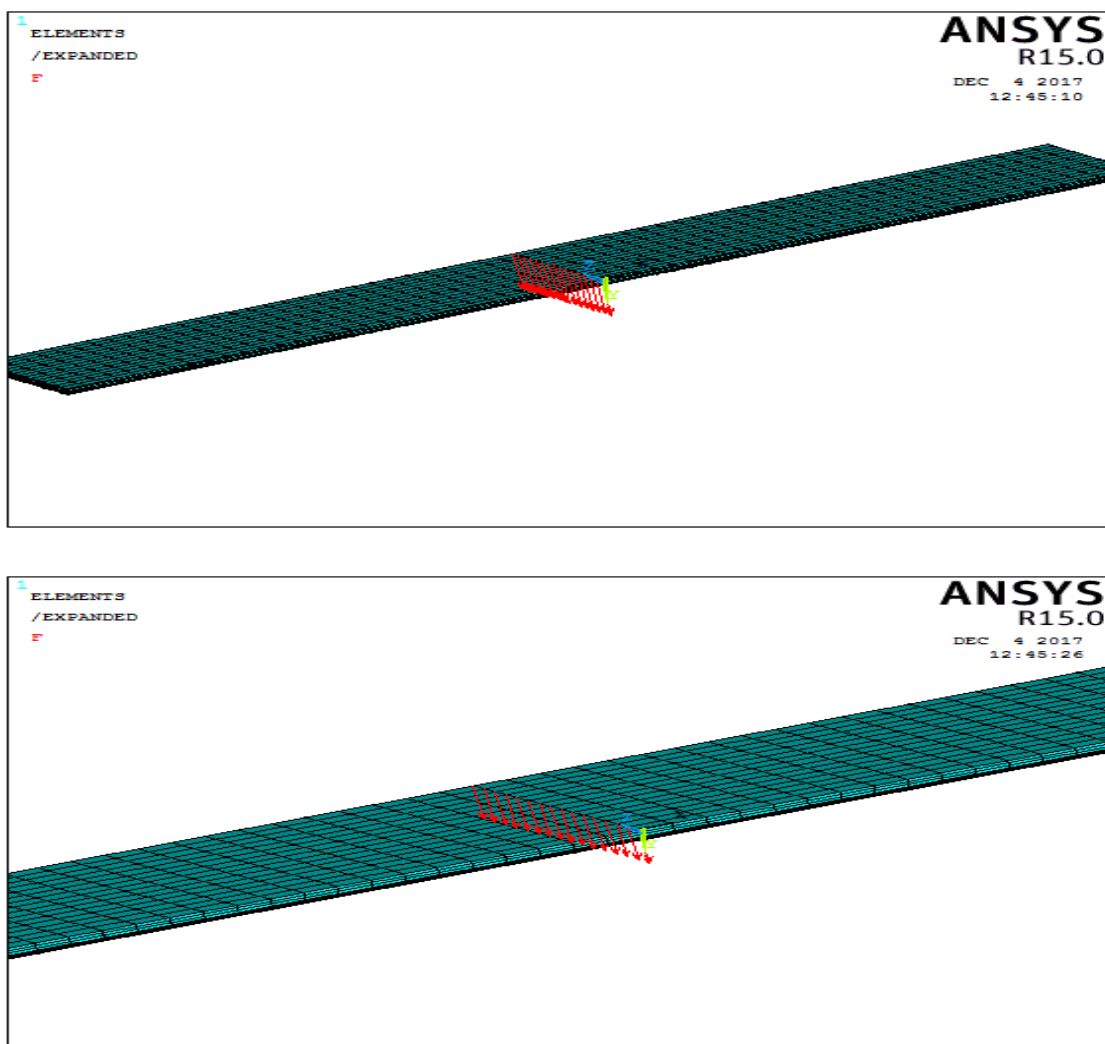


Figure 4. 8: Define load applying

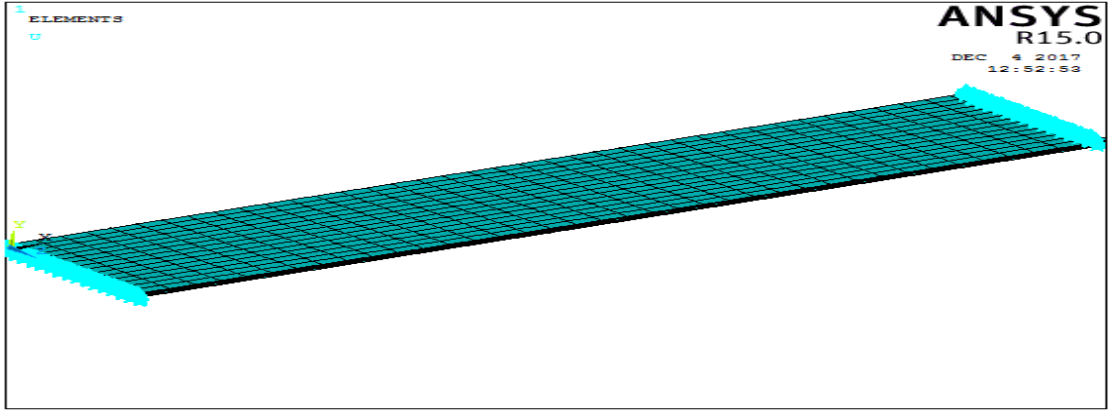


Figure 4. 9: Define Boundary Condition

CHAPTER FIVE

RESULTS AND DISCUSSION

5.1 Introduction

This chapter consists mainly of two sections. The first one is interested with the preparation of material parameters based on the experimental tests of the present study. This section focuses on experimental results of present work which will be discussed in details by the figures and tables. It includes preparation of aluminum alloy samples, polymer (epoxy resin), one as a pure and other as a matrix reinforced with different ratios of (fly ash) powder.

A lot of specific tests have been performed on the all prepared samples to know the properties of this material, all the experimental results are obtained from the mechanical tests (bending test, tensile test and roughness test).

The second section of this chapter is concerned with performing the finite element method. Finite element model is constructed to match the geometry and physical properties of the coated samples. The processes are achieved by using finite element package ANSYS ver. 15. The revealed results are compared to that obtained from the experimental work to verify the accuracy of the suggested model.

5.2 Tensile Test Results of Used Materials

5.2.1 Tensile Test results of aluminum alloy

Different mechanical properties were tested on the prepared samples of aluminum alloy and the results were obtained by conducting tensile tests on the prepared samples using Universal Testing Machine, Table 5.1 shows mechanical properties of aluminum alloy.

Table 5. 1: Mechanical properties for Aluminum alloy

Elastic modulus (GPa)	Upper yield strength (MPa)	Lower yield strength (MPa)	Tensile strength (MPa)
12.9	153	3	163

5.2.2 Tensile Strength Results of epoxy material

Table 5.2 shows the tensile strength of epoxy and mechanical properties of it, the results obtained by using Universal Testing Machine.

Table 5. 2: Mechanical properties for epoxy resin

Break distance mm	Total elongation	Tensile strength MPa	Elastic modulus MPa
3.32	6.2%	28	2800

5.2.3 Tensile Strength Results of epoxy with fly ash

Various mechanical properties were tested on the prepared samples of epoxy with difference of fly ash ratio. The results were obtained by conducting tensile tests on the prepared the composites materials using Universal Testing Machine. According to Table 5.3. The tensile strength increases progressively with increasing wt. % of fly ash level from 1% up to a maximum value at 3%, the Figure 5.1 shows an effect of different percentage content of fly ash particles reinforcement phase on the tensile strength. In this case addition of fly ash particles reinforcement to epoxy matrix increases tensile strength of nanocomposite materials referred to strong interface between the phases that distributes and transfers the load from the matrix to the reinforcement resulted in tensile strength improvement.

Table 5. 3: The results of tensile strength after the addition of different Fly ash ratios

Sample Epoxy: Fly ash	Tensile strength MPa	Elastic modulus MPa
99 :1	35	3500
98:2	42	5500
97:3	55	7600

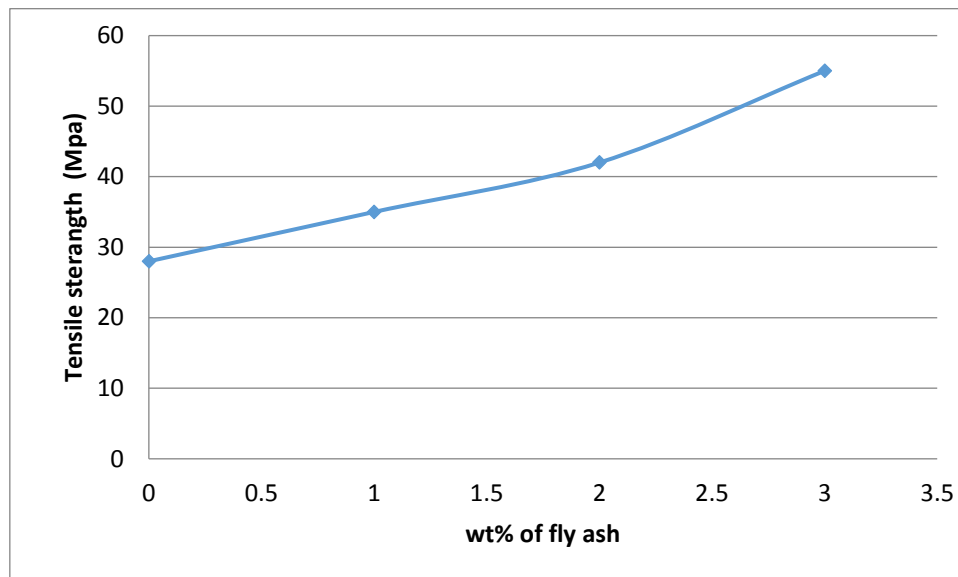


Figure 5. 1: The relationship between tensile strength and percentages weight of fly ash powder additives

5.3 Bending Test Results

5.3.1 Bending test results of aluminum samples coated without the surface roughness

From bending test and according to the relationship (using the relationships (2.1) and (2.3)) of flexural strength and maximum shear stress of aluminum alloy coated with a polymer (pure epoxy resin and epoxy with (fly ash, 1%, 2% and 3% wt. of epoxy), the variations of flexural strength and the maximum shear stress of aluminum sample are as a function of Figure 5.2 and Figure 5.3. These figures indicate that the sample of aluminum (A1) coated with a polymer layer (pure epoxy) has a higher flexural and maximum shear stress than the samples of aluminum (A2, A3 and A4) coated with a polymer (epoxy with fly ash in different ratios). It

is also shown that the added value of fly ash material to polymer coating layer decreases the flexural strength and the maximum shear stress values on these samples. It is possibly produced by an incompatibility of the fly ash particles and the polymer matrix, leading to weak interfacial bonding. Fly ash particles formed bunch or agglomerate among themselves result in a filler-filler interaction due to the strong polarity of hydroxyl collections on the fly ash surfaces that results in weak interfacial bonding.

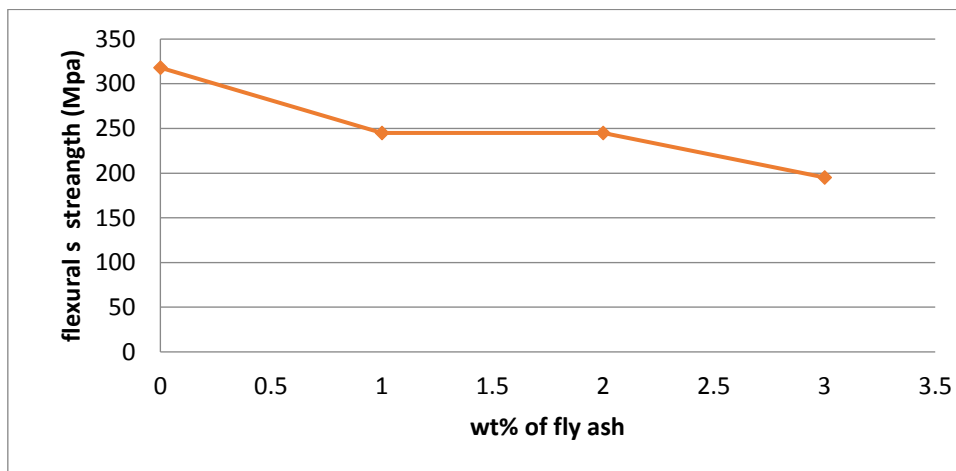


Figure 5. 2: The flexural strength of aluminum coated as a function of wt. % of fly ash content in the epoxy coating layer without surface roughness surface

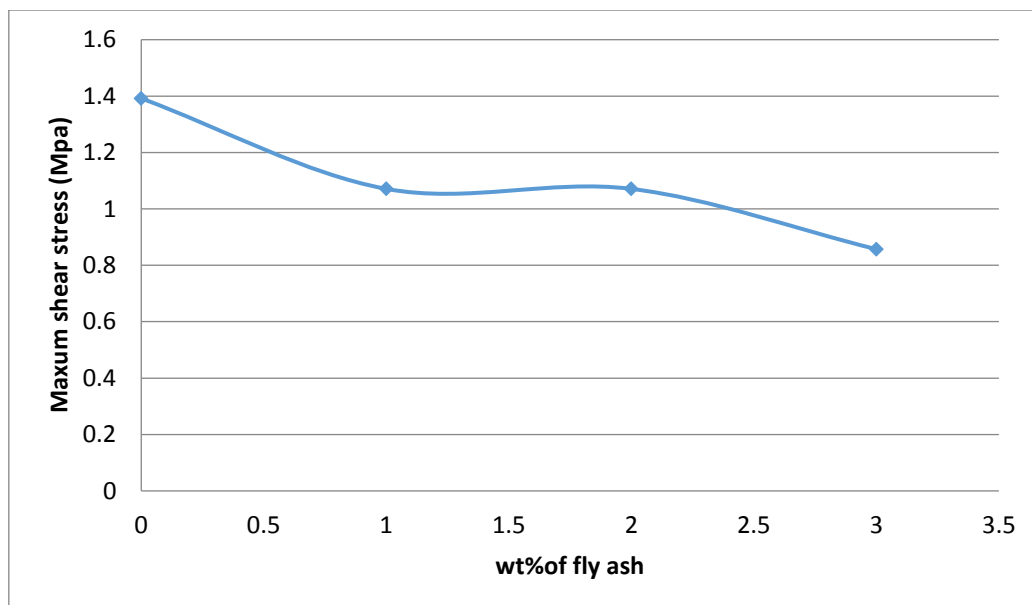


Figure 5. 3: The maximum shear stress of aluminum coated as a function of wt. % of fly ash content in the epoxy coating layer without surface roughness

5.3.1.1 Elongation at Break in the Experimental and Numerical Simulation

The comparison of elongation at fracture in bending test for (A1), (A2), (A3) and (A4) samples of aluminum alloy coated by polymer with zero surface roughness in experimental and numerical simulation tests and the error percentage were done on final model prepared for this study by using ANSYS package, experimental work was conducted in this study to investigate the bending test on the same samples. Numerical analyses and experimental results are compared for bending test is shown in Figure 5.4 and Table 5.4.

Also, the elongations of samples with dimensions (120×20×0.7) mm for aluminum substrate while the dimensions of polymer coating are(120×20×0.3)mm were calculated after bending test, in numerical simulation are shown in Figure 5.5 (a, b, c and d).

Table 5. 4: The maximum elongation at break (mm) in experimental and simulation tests

Sample no	Fly ash ratio%	Elongation (mm) at experimental	Elongation (mm) at simulation	Error percentage %
A1	0	12	11.77	1.91
A2	1	18	19.89	10.5
A3	2	30.5	31.97	4.81
A4	3	34	34.32	0.94

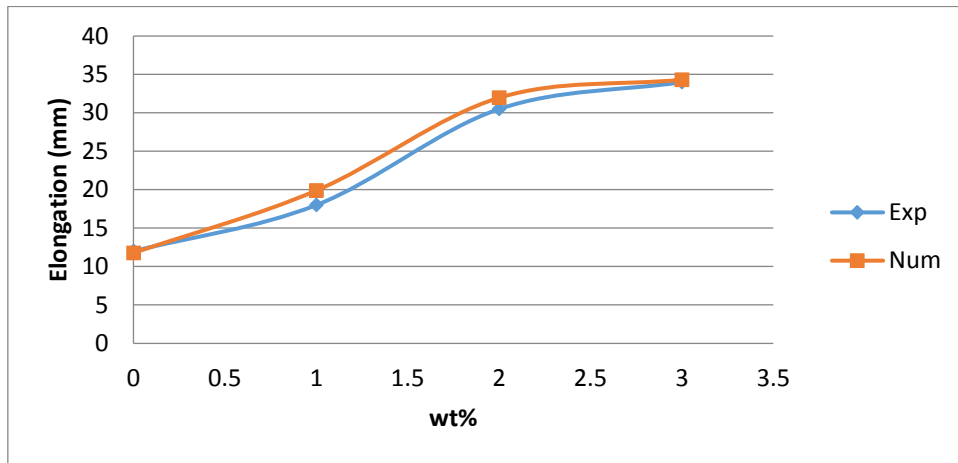
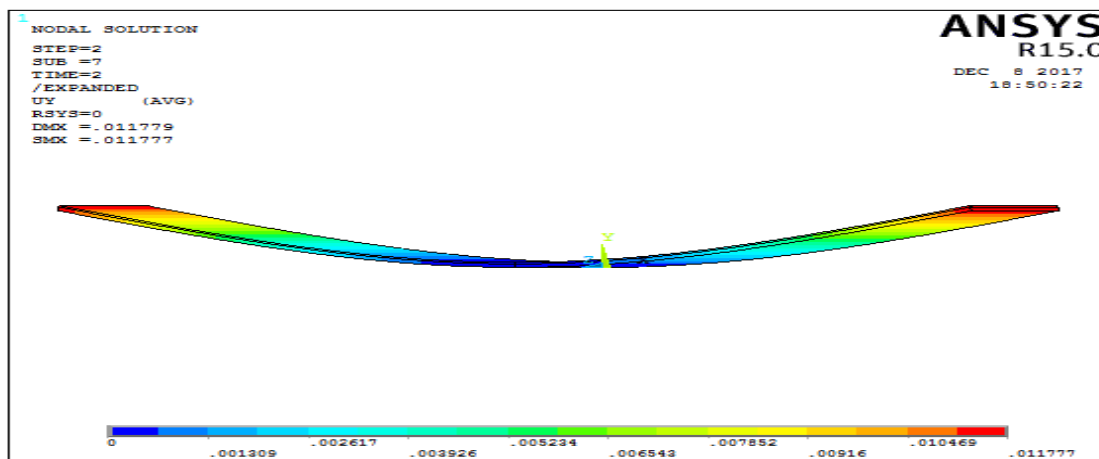
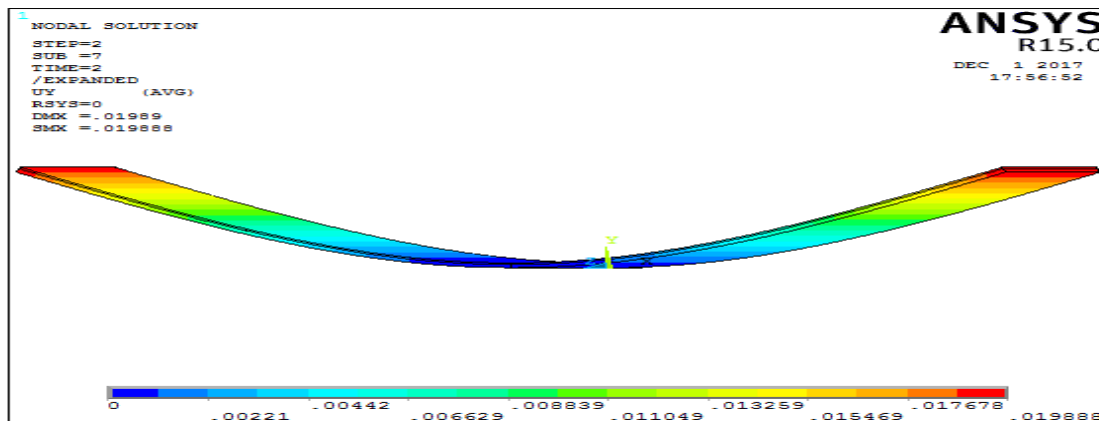


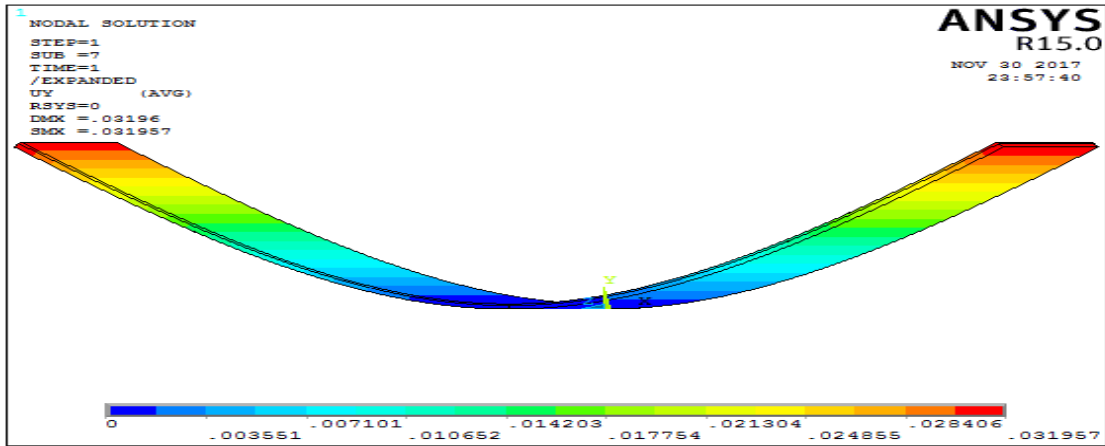
Figure 5. 4: Comparison the elongation (mm) of aluminum alloy samples (A1, A2, A3 and A4) coated by polymer without surface roughness of product in the numerical and experimental tests



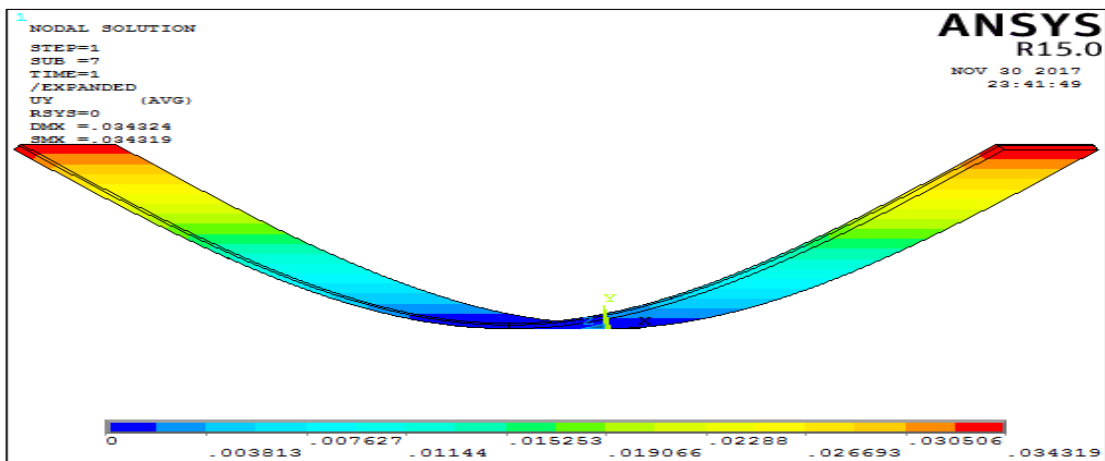
a) sample at pure epoxy without the surface roughness



b) sample at epoxy with(1%) of fly ash powder without the surface roughness



c) sample at epoxy with(2%) of fly ash powder without the surface roughnees



d) sample at epoxy with(3%) of fly ash powder without the surface roughnees

Figure 5. 5: (a,b,c and d) shows elongation at break in aluminum alloy coated by epoxy with different weight percentages of fly ash under bending test in the numerical simulation

According to Table 5.4 and Figure 5.4 and Figure 5.5, the elongation at break for two types of tests, increased with increasing adding wt. % of fly ash. Observation is attributed to increasing in crosslink density with increasing wt. % of fly ash leading to a drop in molecular chain mobility and the effect of fly ash nanoparticles on the properties of the polymer material for improving elongation of the samples.

The comparison of results according to Table 5.4 lists the error percentage between the numerical and experimental work are (1.91%, 10.5%, 4.81% and 0.94%) respectively.

5.3.2 Bending results of the aluminum samples coated with the surface roughness

The relationship (by using the equation (2.1) and (2.3)) of flexural strength and maximum shear stress of aluminum alloy coated with polymer (pure epoxy resin and epoxy with (fly ash, 1, 2, and 3 wt. % of epoxy)) at three different degree of the surface roughness (100 grit, 320 grit and 600 grit) is indicated in Figures 5.6 and Figure 5.7.

These figures shows that the specimens with surface roughness (600 grit) have a higher flexural strength and maximum shear stress than the other specimens by surface roughness (100 grit) and by (320 grit), the bending strength and maximum shear stress are decreased when the surface roughness is increased this caused by the adhesive force are increased as roughness are get higher.

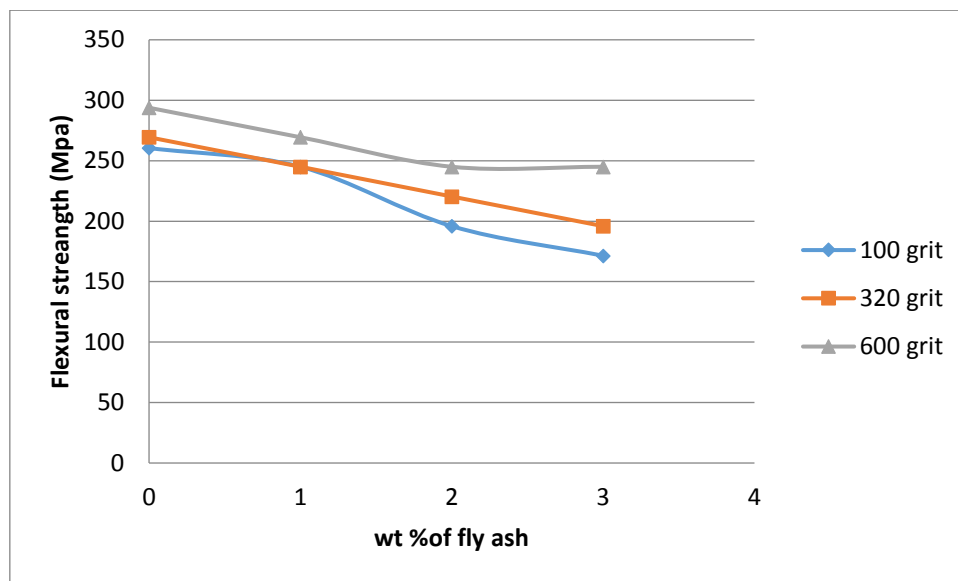


Figure 5. 6: The flexural strength of aluminum samples coated as a function of the surface roughness content in the epoxy coating layer with variation ratios of fly ash

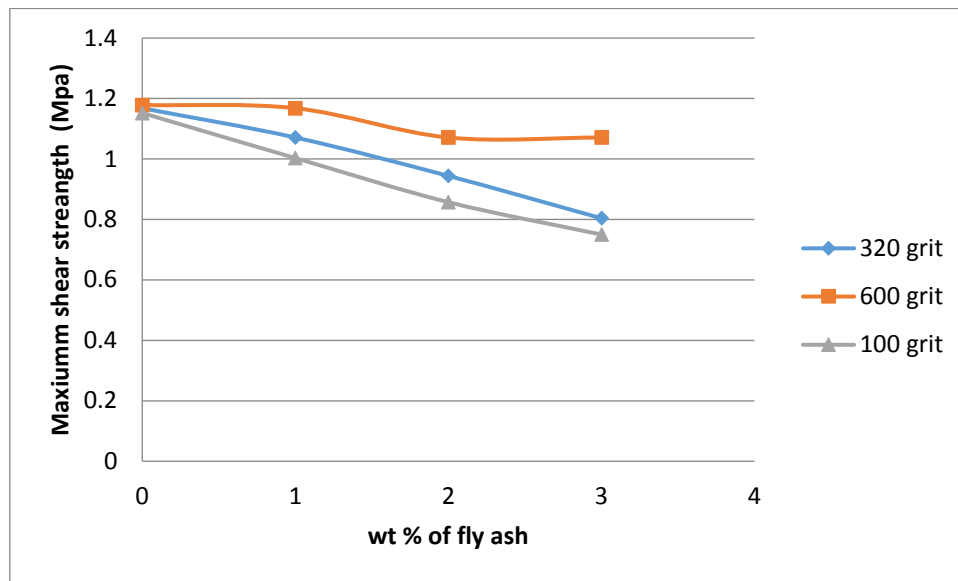


Figure 5. 7: Maximum shear strength of aluminum samples coated as a function of the surface roughness content in the epoxy coating layer with (wt. % of fly ash)

5.3.2.1 Elongation at Break in Experimental and Numerical Simulation

The same procedure of numerical and experimental elongation test done on aluminum samples without surface roughness will be done on samples of same dimension with surface roughness of different ratios (100,320,600) grit.

Figure 5.8, Figure 5.10, and Figure 5.12, and Table 5.5, Table 5.6, and Table 5.7 describe the relation for the experimental and numerical simulation results, for roughness aluminum surface. The results of these tests showed that as the ratio of fly ash and roughness is increased, the elongation of coating was increased so the largest elongation was get it at 100 grit. The reason for increasing elongation with roughness is that the coherence force between substrate and coating layer with fly- ash are increment which allow to coating to stretch. Reported factors above will also improve adhesive force between materials used in recent study.

Table 5. 5: The maximum Elongation (mm) in the experimental and simulation test of the samples (B1, B2, B3 and B4) with roughness (100 grit)

Sample no	Fly ash ratio%	Elongation (mm) at experimental Test	Elongation (mm) at simulation Test	Error percentage %
B1	0	33.5	35.32	5.4
B2	1	37.5	36.37	3
B3	2	48	48.99	2.1
B4	3	51	54.18	6.2

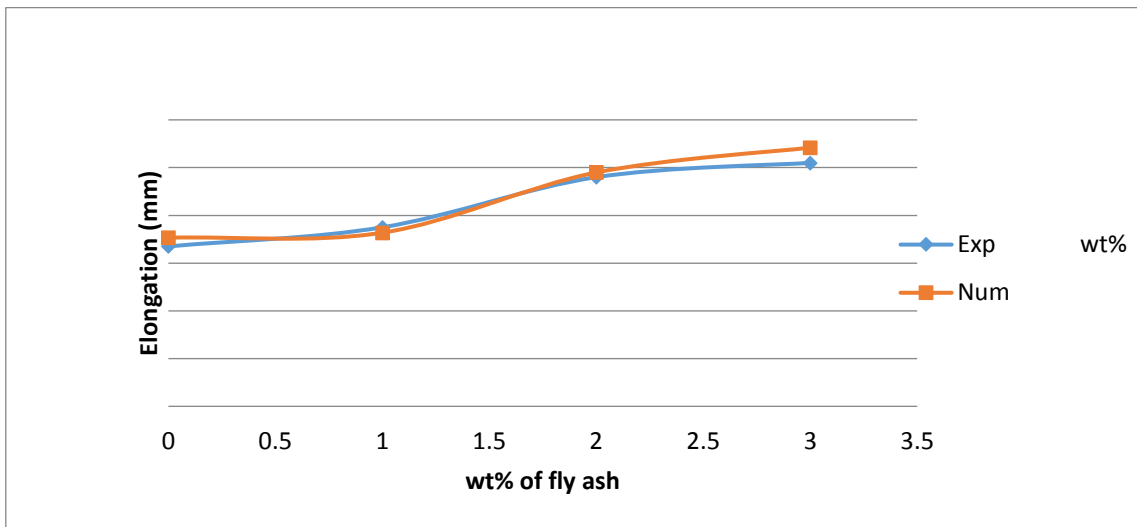
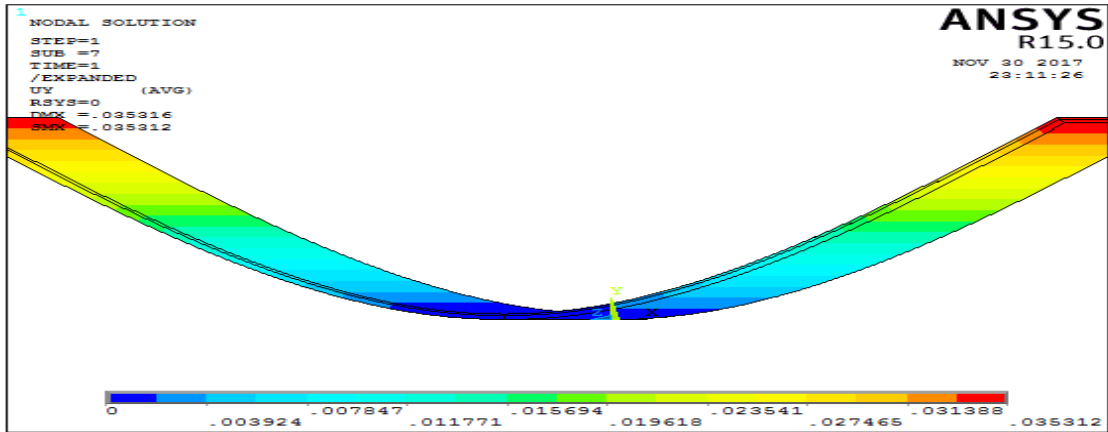
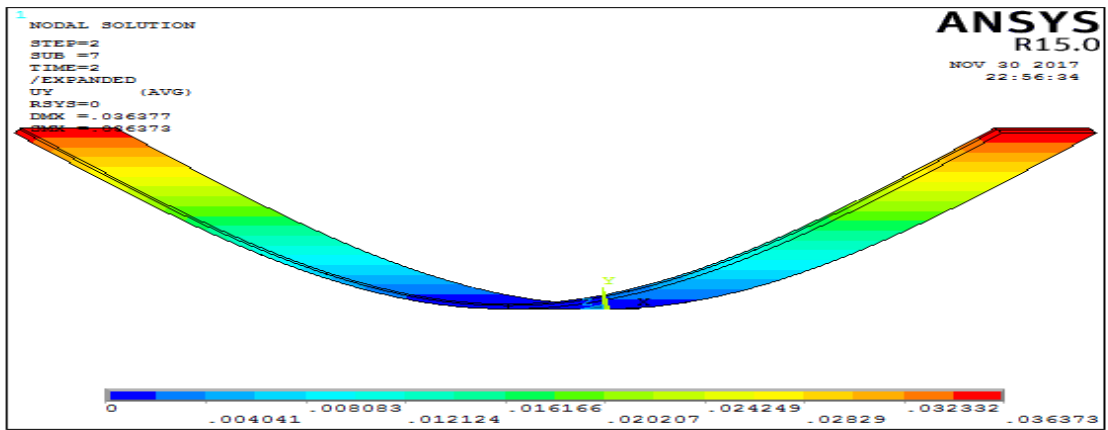


Figure 5. 8: Comparison between numerical and experimental elongation (mm) of the (B1, B2, and B3 and B4) samples

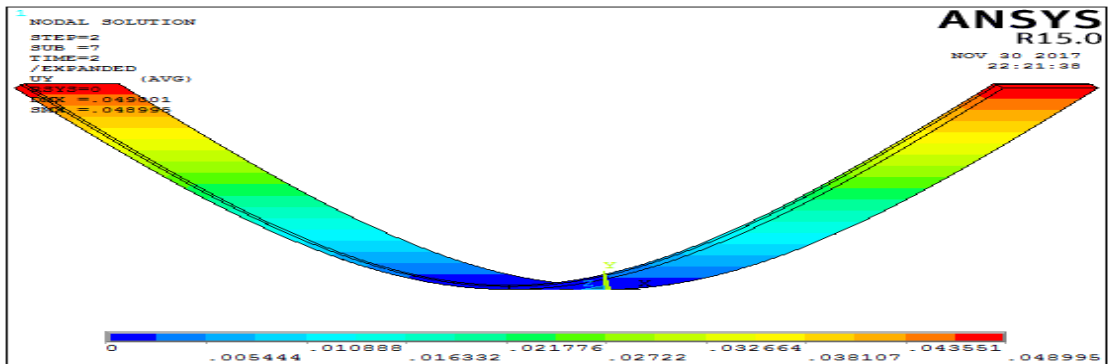
Figure 5.9 , Figure 5.11 and Figure 5.13 show the maximum elongation of aluminum alloy samples of dimensions(120×20×0.7)mm coated by polymer layer of dimensions (120×20×0.3)mm with surface roughness (100 grit ,320grit and 600 grit) by using the numerical analysis.



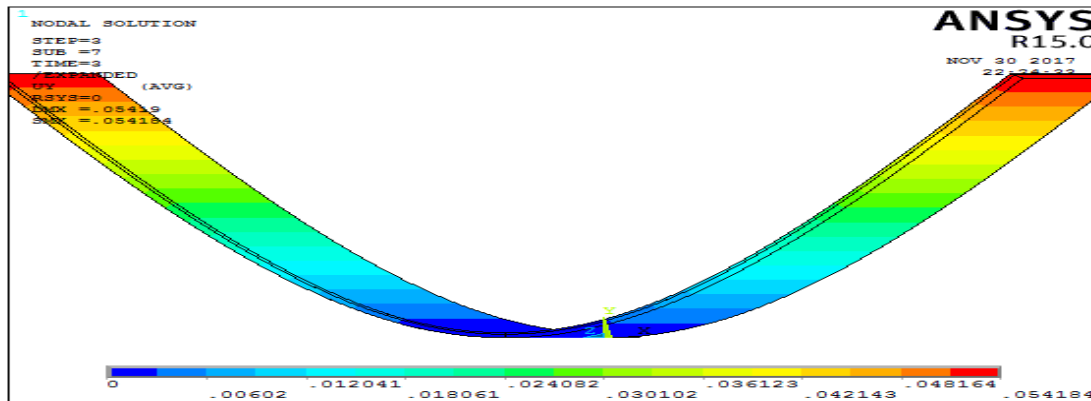
a) The sample at pure epoxy with surface roughness (100)grit



b) Sample at epoxy with (1%) of fly ash powder with surface roughness(100)grit



c) sample at epoxy with (2%) of fly ash powder with surface roughness(100)grit



d) Sample at epoxy with(3%) of fly ash powder with surface roughness(100)grit

Figure 5. 9: (a,b,c and d) shows the elongation in the aluminum alloy coated by epoxy with different wt% of fly ash under bending test in numerical analysis

Table 5. 6: The maximum Elongation (mm) in the experimental and simulation tests of the samples with roughness (320 grit)

Sample no	Fly ash ratio%	Elongation (mm) at experimental	Elongation (mm) at simulation	Error percentage
C1	0	17.6	14.88	15.40
C2	1	24	21.86	8.9
C3	2	39.5	40.136	1.61
C4	3	41.5	41.7	0.48

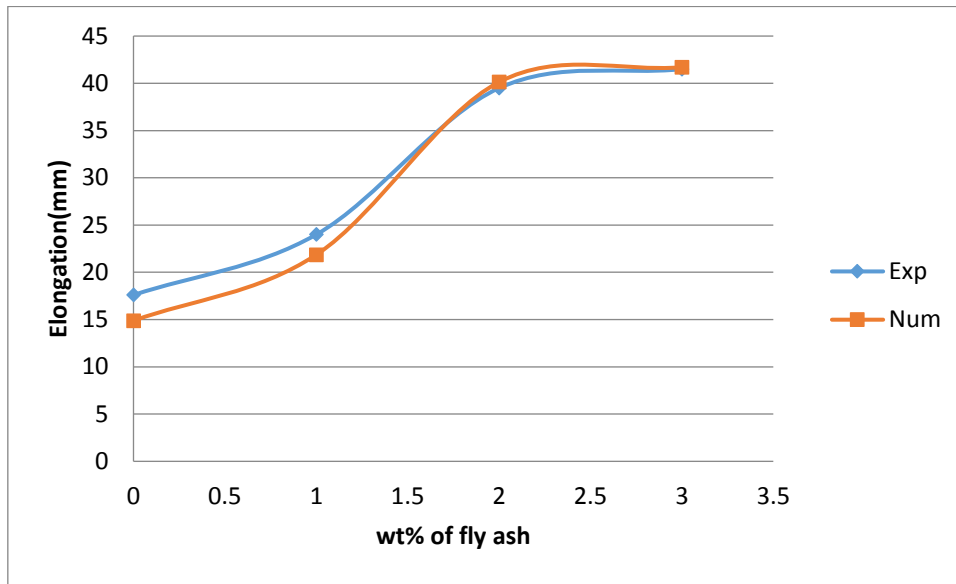
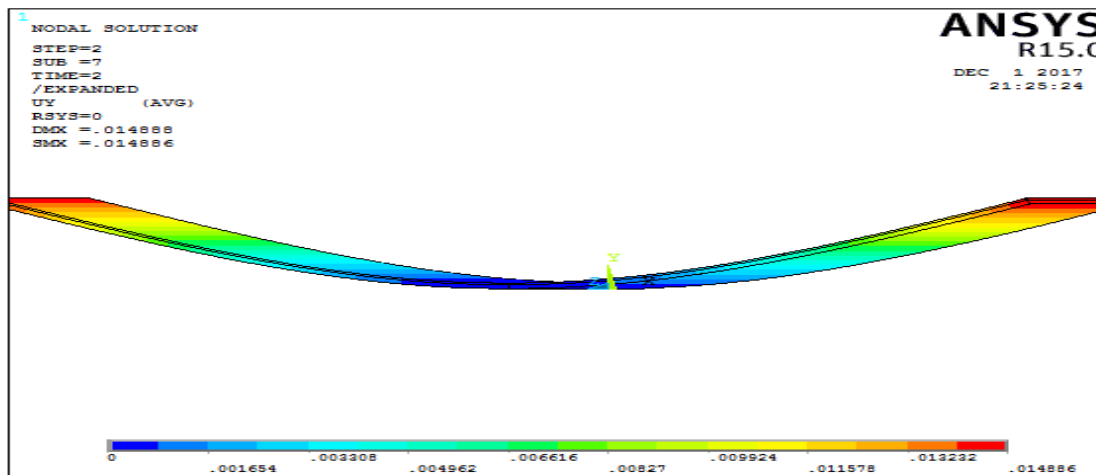
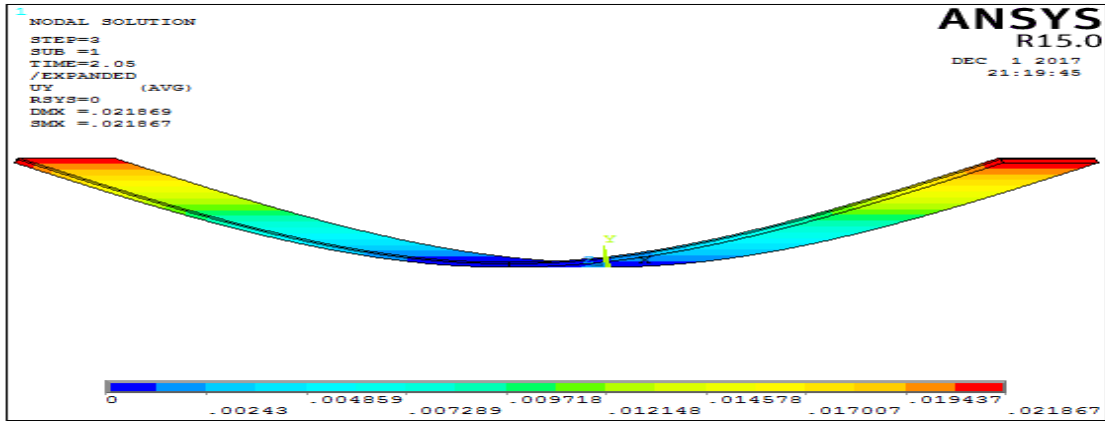


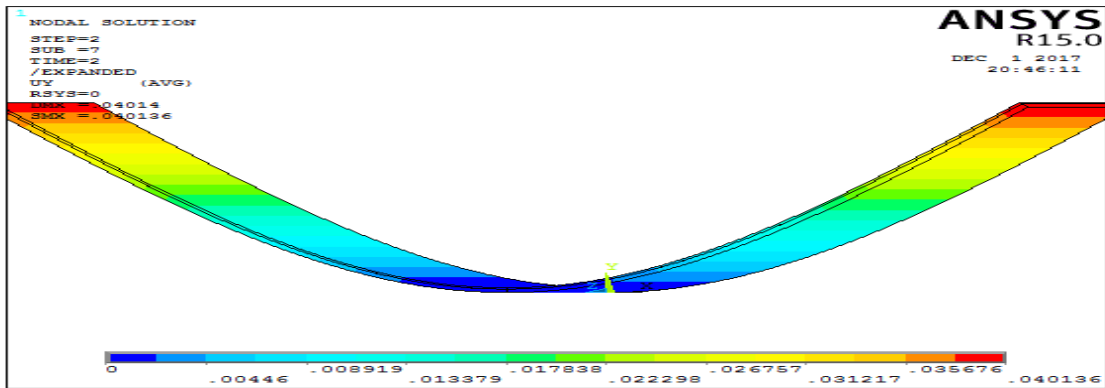
Figure 5. 10: Comparison between numerical and experimental to the elongation (mm) of the (C1, C2, and C3and C4) samples



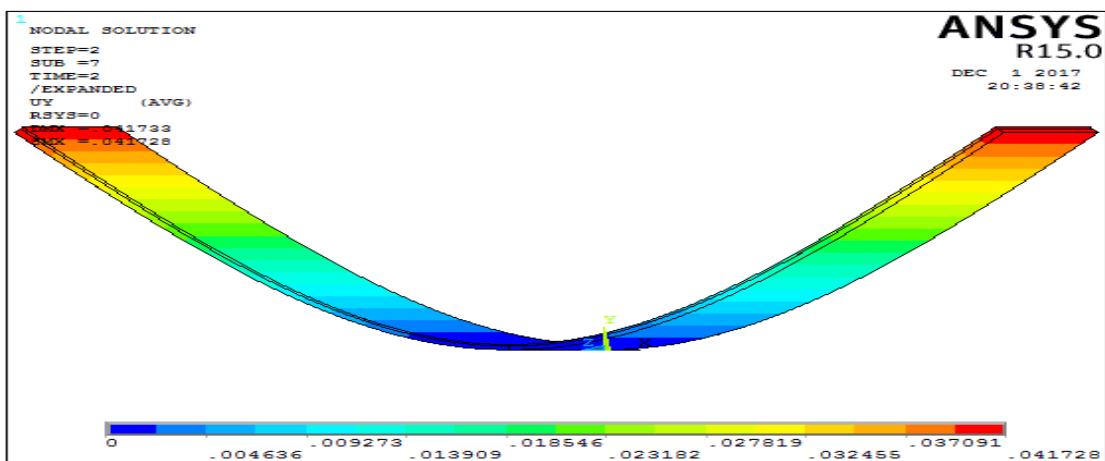
a) sample at epoxy with (0%) fly ash powderwith the surface roughnees (320) grit



b) sample at epoxy with (1%) fly ash powder with the surface roughness (320) grit



b) sample at epoxy with (2%) fly ash powder with the surface roughness (320) grit



d) sample at epoxy with (3%) fly ash powder with the surface roughness (320) grit

Figure 5. 11: (a,b,c and d) shows elongation in aluminum alloy coated by epoxy with different wt% of fly ash under bending test by using the numerical analysis

Table 5. 7: The maximum Elongation (mm) in the experimental and simulation tests of the samples with roughness (600 grit)

Sample no	Fly ash ratio%	Elongation (mm) at experimental	Elongation (mm) at simulation	Error percentage %
D1	0	9.92	11.179	12.6
D2	1	17	17.415	2.4
D3	2	33.8	30.588	9.5
D4	3	40	37.47	6.3

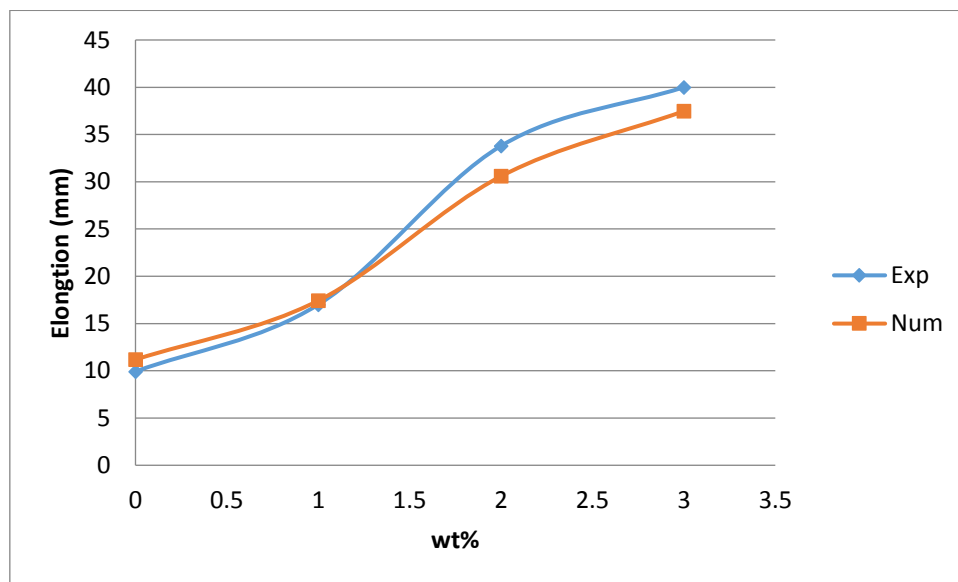
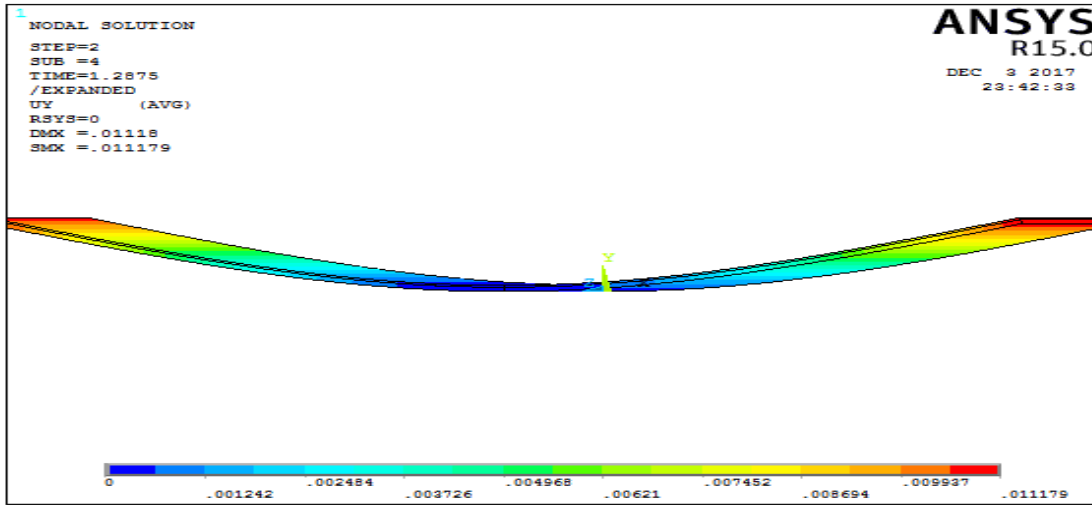
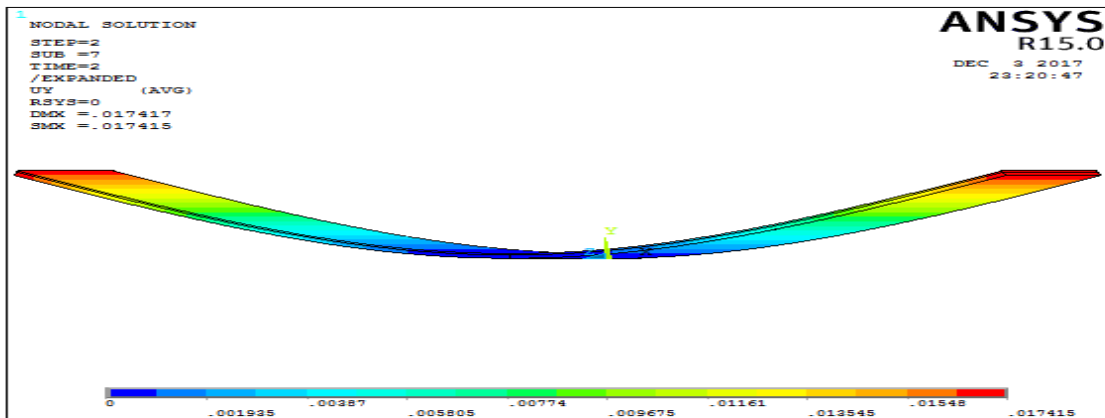


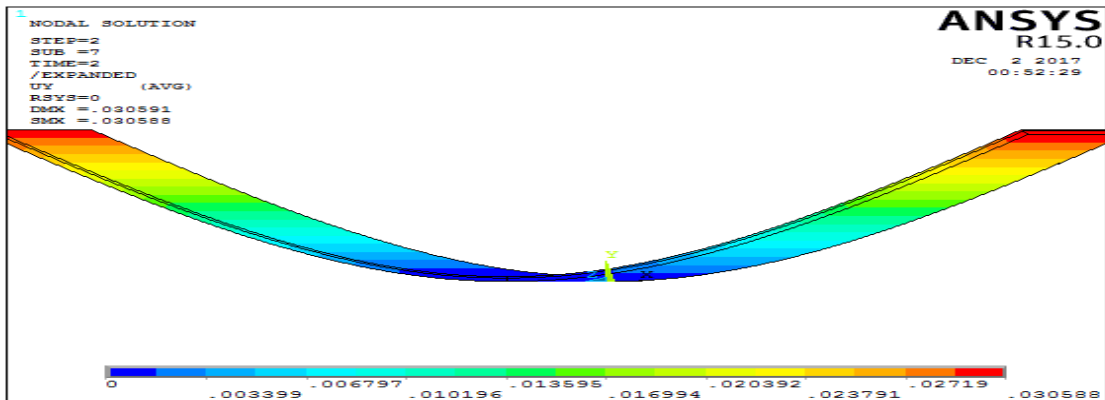
Figure 5. 12: Comparison between numerical and experimental elongation (mm) of the (D1, D2, and D3 and D4) samples



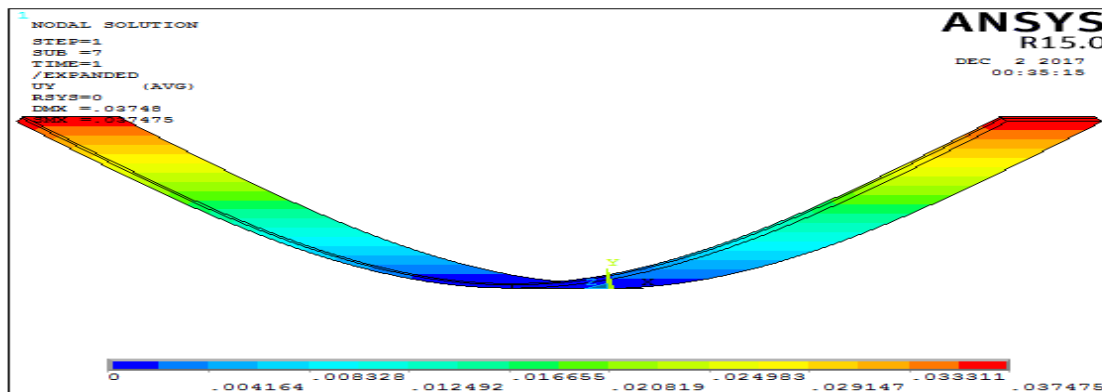
a) sample at epoxy with (0%) of fly ash powder with the surface roughnees (600) grit



b) sample at epoxy with (1%) of fly ash powder with the surface roughnees (600) grit



c) sample at epoxy with (2%) of fly ash powder with the surface roughnees (600) grit



d) sample at epoxy with (3%) of fly ash powder with the surface roughness (600) grit

Figure 5. 13: (a,b,c and d) shows the elongation in the aluminum alloy coated by epoxy with different wt% of fly ash under bending test by using the numerical analysis

Also, the comparison results according to Table 5.5, Table 5.6 and Table 5.7 show the error percentage between the numerical and experimental work are (5.4%,3%,2.1%, and 6.2%,) at 100 grit , (15.4%, 8.9%,1.61%, and0.48%,) at 320 grit and ,(12.6%, ,2.4%,9.5% and6.3 %) at 600 grit respectively and tables show that the error percentage between the two tests is trivial.

According to the numerical results in Figure 5.9, Figure 5.11 and Figure 5.13 show that the elongation is get greater when the added value of fly ash and surface roughness are increased depending on the mechanical properties obtained from the tensile test of the samples made of (aluminum alloy, epoxy resin and epoxy with fly ash in different values).

And that indicates the success of the curriculum followed in the experimental and simulation procedures therefore, F.E.M program can be adopted for other tests.

5.4 Drop Test

As the experimental results obtained from aluminum sheet painted by epoxy with fly ash ,the bending test results are closest to results obtained from the tests in ANSYS computer program, then to reduce the cost of making practical experiment every time, the using of ANSYS program is cheaper and appropriate instead of practical experiments.

Drop Test, It is one of these practical experiments. It is suitable to use ANSYS with assumptions of using a steel ball with (5) mm radius dropped in speed of (50 m/sec) to conflict

the painted side of plate to study the impact speed with the painted layer before and after addition of fly ash in previously mentioned ratios. The model test as shown in Figure 5.14 and Table 5.12 show the properties of the steel ball.

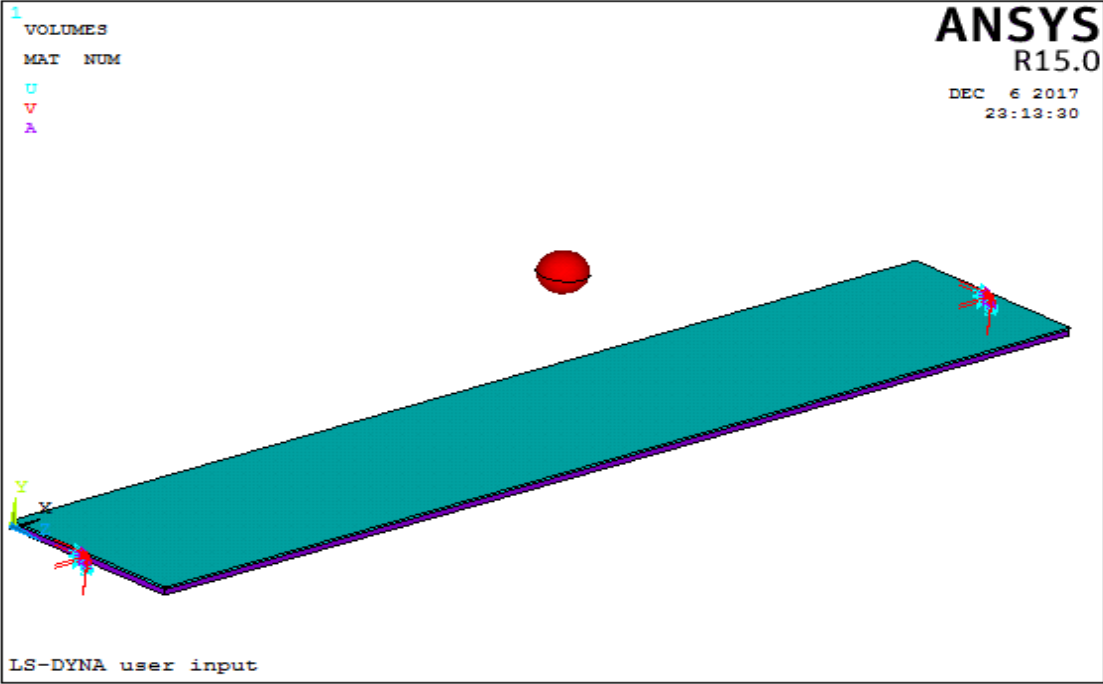


Figure 5. 14: The model of Drop test

Table 5. 8: The properties of the steel ball

Tensile strength (Mpa)	165
Elastic modulus (Gpa)	200
Passion ratio	0.3

Figure 5.15, Figure 5.16, Figure 5.17 and Figure 5.18, present the effect of added value of fly ash to polymer which is incrementing the value of damping speed, so the change in the

shock resistance and the absorption of speed is very slight, where it was observed that(50 m/s) speed has damped only (13 m/s) if the aluminum alloy coated by pure epoxy ,and a speed of aluminum alloy coated by polymer with (epoxy of 1% fly ash)was damped(16.3262 m/s) from (50 m/s) while the speed of the aluminum alloy coated with(epoxy of 2% fly ash) has damped from (50 m/s) about (17.1269 m/s). The last sample of aluminum alloy coated by polymer (epoxy of 3% fly ash) the speed is damped (17.91 m/s), from (50 m/s).

The interaction between polymer and fly ash particle produces energy this energy absorbs droop speed energy as mentioned. As the ratio of add fly ash increased then the capability of speed damping is increased i.e. the impact resistance of material is incremented with incremented the added value of fly ash.

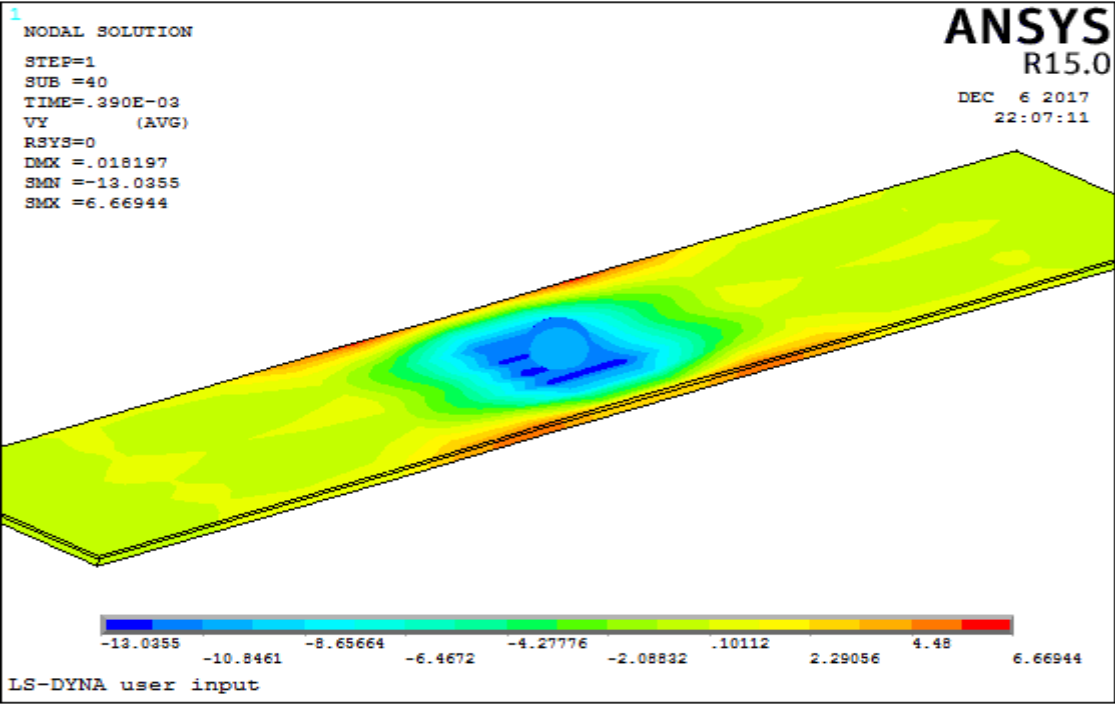


Figure 5. 15: Drop test of Aluminum alloy coated by epoxy

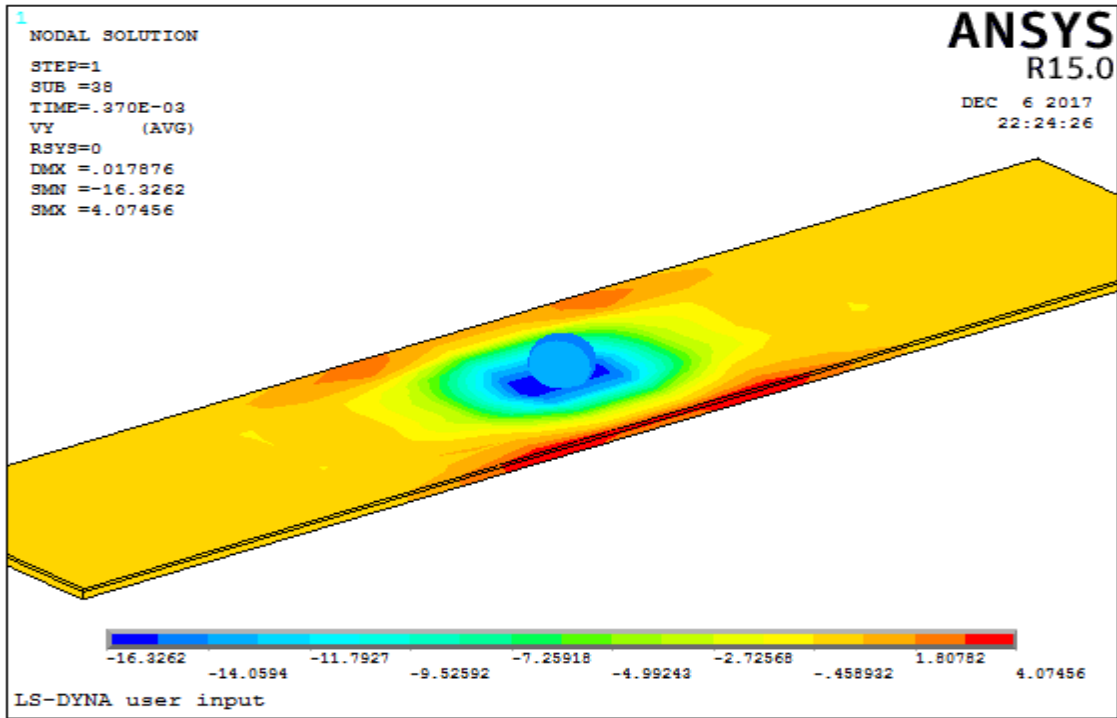


Figure 5. 16: Drop test of Aluminum alloy coated by epoxy with 1% fly ash

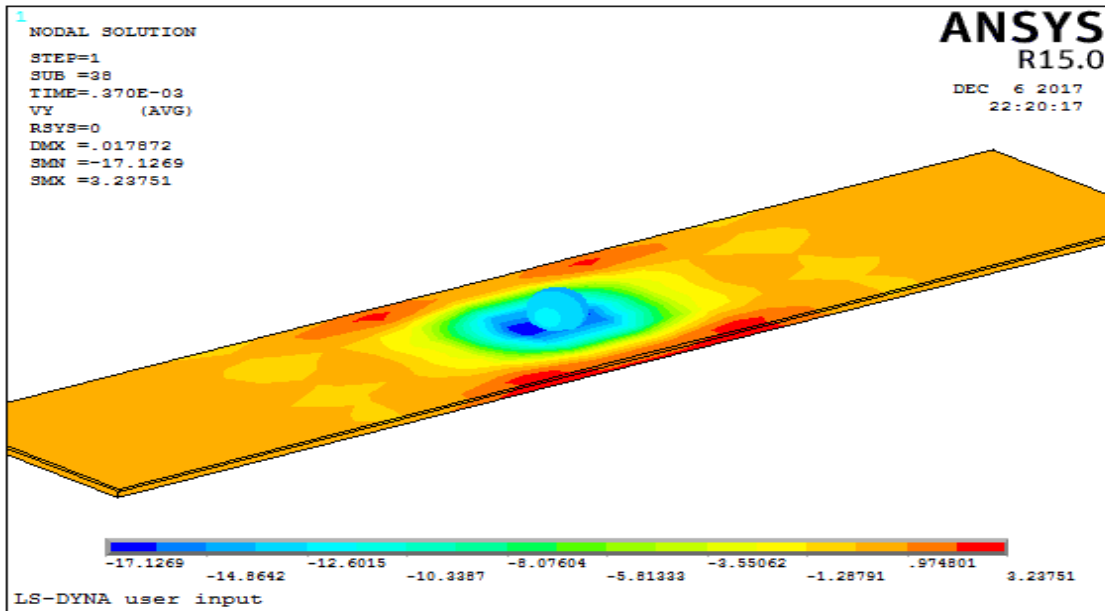


Figure 5. 17: Drop test of Aluminum alloy coated by epoxy with 2% fly ash

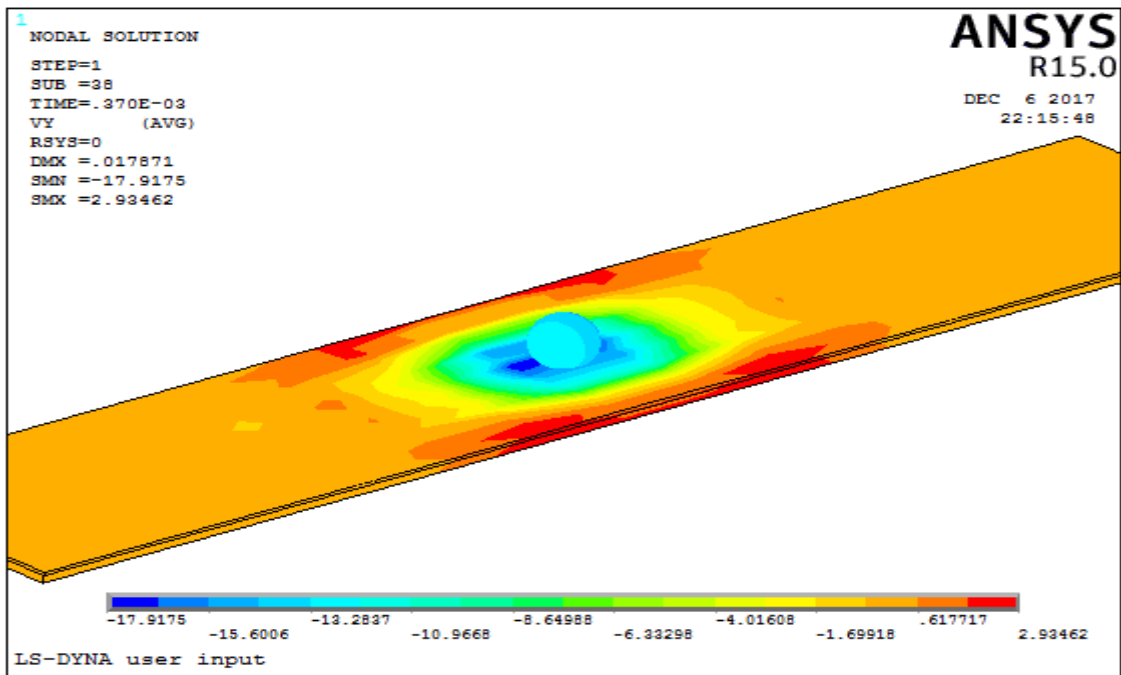


Figure 5. 18: Drop test of Aluminum alloy coated by epoxy with 3% fly ash

CHAPTER SIX

CONCLUSION AND RECOMMENDATION

6.1 Conclusions

In the present work, attempts are made to improve polymer coating of aluminum alloy by coating the samples with polymer composite material with epoxy based matrix and nanoparticle (fly ash) as a reinforcement material, and bending of the sheet, being an important parameter, are considered in this set-up. Experiment is followed by numerical simulations using Finite Element Analysis package (15). The summary and conclusions from experiments and numerical simulations are summarized below:

1. Tensile strength increases progressively with increasing wt. % of fly ash level from 1% up to a maximum value at 3%, while the best tensile strength was at 3wt% of fly ash.
2. The addition of fly ash material to the polymer coating layer of the aluminum alloy samples without surface roughness decrease the flexible strength and the maximum shear stress values ,while the pure epoxy showed higher flexible stress and maximum shear stress.
3. Flexible strength and maximum shear stress decrease progressively with increasing wt. % of fly ash level and surface roughness(100 grit, 320 grit and 600 grit), of the aluminum alloy samples by polymer coating layer .
4. The results of tests showed that as percentage ratio of fly ash is increased, the elongation of coating was increased also for all samples of aluminum alloy coated with different ratios of fly ash .It is also noted the coating layer prepared from 3%wt of fly ash with epoxy resin has higher (elongation and adhesive force) compared with other coatings by polymer composite material layer.
5. The elongation is increased with increment of surface roughness at (100grit) for all the samples. And, the lower value of elongation was showed with the samples of surface roughness (600 grit).
6. Observed from experiments that the differences in results between the experiments and numerical analysis are closest, and that indicates the success of the curriculum followed

in the experimental and simulation procedures therefore, a program can be adopted for other tests.

7. The drop test, are carried out by simulation whereas the additions of fly ash increase the damping value of speed also is increased.
8. Numerical simulations which can be used to lessen time, cost and finally recover the product quality.

6.2 Recommendations for Forthcoming Work

- 1- This work leaves a widespread scope for future research. The composites of similar nature can be tasted for diverse mechanical behavior. Thermoplastic also can be used apart from thermoset polymers as the matrix material.
- 2- Study the effect of other nanoparticles as (CeO, ZnO, Al₂O₃,and TiC) on the microstructure and mechanical properties materials.
- 3- Study the wear characteristics of polymer materials.
- 4- Study the effect of material properties and detailed study of the stress distribution in the polymer coatings by using numerical simulation.

REFERENCES

1. Cleveland, Ohio, 1996, Coil Coating, Technical Bulletin, National Coil Coating Association.
2. Altenpohl D.G., 1998, Aluminum: Technology, Applications, and Environment, The Aluminum Association Inc. and TMS,
3. Hatch J.E., 1984, American Society for Metals, Aluminum: Properties and Physical Metallurgy.
4. Lodhi, Veerendra Singh; Jain, 2014, a Review of Experimental Study of Spring Back Effect of Aluminum Sheet Metal.
5. Ulrich-Andreas Hirth, 2005, Aluminum Pigments for Powder coating Applications, Paper V.3 from the 8th Nürnberg Congress.
6. Bentley, J. & Turner, G.P.A., 1997, Introduction to paint chemistry and principles of paint technology, CRC Press.
7. Hibbeler, R., 2005, CSI second edition, Prentice Hall, Mechanics of materials.
8. Kailas, S. V, 2011, Materials Science. Journal of Mechanics of Materials and Structures.
9. Saha P.K., 1993, Boundary friction measurements in sheet metal forming," Ph.D. dissertation, University Microfilms International, Ann Arbor, MI.
10. A. Azushima and M. Sakuramoto, 2006, Effects of plastic strain on surface roughness and coefficient of friction in tension-bending test, CIRP Annals-Manufacturing Technology.
11. N. Panich, P., Wangyao, T., Chomtohsuwan, and S. Yong, 2006, Finite element analysis of the critical ratio of coating thickness to indentation depth of soft coating on a harder substrate by Nano indentation," Science Asia, pp. 411-416.
12. M. Wong, G.T. Lim, A. Moyse, J.N. Reddy, and H.J. Sue, 2004, a new test -ology for evaluating scratch resistance of polymers" Wear, vol. 256, no. 11-12, pp. 1214-1227.
13. J.S.S. Wong, H.J. Sue, K.Y. Zeng, R.K.Y. Li, and Y.W. Mai, 2004, Scratch damage of polymers in nanoscale," Acta Materialia, vol. 52, no. 2, pp. 431-443.
14. Bajata J.B., V.B. Mišković-Stankovića Z., 2008, Corrosion stability of epoxy coatings on aluminum pretreated by vinyltriethoxysilane, Faculty of Technology and Metallurgy, University of Belgrade.

15. Toshiyasu Nishimura and Vedarajan Raman, 2015, Epoxy polymer coating to prevent the corrosion of aluminum nanoparticles. John Wiley & Sons, Ltd.
16. Tullio Monetta, Annalisa Acquesta and Francesco Bellucci, Graphene Epoxy Coating as Multifunctional Material for Aircraft Structures, Department of Chemical, Materials and Production Engineering, University of Naples Federico II, Piazzale Tecchio 80, 80125 Naples, Italy.
17. Amer Hameed Majeed, Mohammed S. Hamza, Hayder Raheem Kareem, 2012, Effect Of Ading Nanocarbon Black On The Mechanical Properties Of Epoxy, Dept. of Material Engineering, College of Engineering, Al-Mustansiriya University Dept. of Material Engineering, University of Technology Dept. of Material Engineering, College of Engineering, Al-Mustansiriya University.
18. A Pattanaik¹, S K Bhuyan¹, S K Samal¹ , A Behera¹ & S C Mishra¹, 2015, Dielectric properties of epoxy resin fly ash composite, Department of Metallurgical & Materials Engineering, National Institute .
19. Nityananda Kalia, 2015, Synthesis And Mechanical Behavior Of Epoxy- Fly Ash Composite, a thesis submitted in partial fulfillment of the requirement for the degree of Bachelor of Technology In Ceramic Engineering
20. W. Shen, B. Jiang, S.M. Gasworth, and H. Mukamal, 2001, Study of tripologica properties of coating/substrate system in micrometer and nanometer scales with a scanning probe microscope," Tribology International.
21. Grainger S. and Blunt J., 1998 Engineering Coatings: Design and Application, Woodhead Publishing Ltd, UK.
22. Emslie A. G., Bonner F. T., and Peck L. G., 1958, Flow of a Viscous Liquid on a Rotating Disk, pp.858-862.
23. Arvind Andre, 2000, Handbook of Plasma Immersion Ion Iplantation and Deposition, New York: Wiley-Interscience .
24. Glocker, David A., and Ismat Shah S., 2002, Handbook of Thin Film Process Technology, Bristol, U.K.: Institute of Physics Pub.
25. I.M. Hutchings and E. Arnold, Tribology, 1992, Friction and Wear of Engineering Materials, Elsevier Limited, London, UK.
26. Nalwa H.S., 1997, Handbook of Organic Conductive Molecules and Polymers”, Wiley, New York.

27. Browning R.L., Jiang H., and Sue H.J., 2008, Scratch behavior of polymeric materials Tribology and Interface Engineering Series.
28. Materials design, 2013, Effect of resin molecular Architecture on Epoxy thermoset mechanical properties, Materials Design.,
29. Pascault H.P. Sauterean H. Ierda J. and Williams R.J., 2002, Thermosetting polymers, Marcel Dekker, New York.
30. Jean Marie Berthelot, 1999, Composite Materials: mechanical behavior and Structural analysis, USA.
31. Satheesh R. R., Maniseka, K. and Manikandan, V., 2013, Effect of Fly Ash Filler Size on Mechanical Properties of Polymer Matrix Composites, International Journal of Mining, Metallurgy & Mechanical Engineering, pp.34-38.
32. Sulaf, M. D., 2010, Preparation of Al-7Si Composite Material Reinforced by Fly Ash and Dust Particles and Studying its Mechanical and Metallurgical Properties, M. Sc. Thesis, University of Technology, Materials Engineering Department, Iraq.
33. Seames, W. S., 2003, An Initial Study of the Fine Fragmentation Fly Ash Particle Mode Generated during Pulverized Coal Combustion, Fuel Processing Technology, pp.109-125.
34. Zhang, X. F., Wang, D. J. and Xie, G., 2002, Manufacturing of Aluminum Fly Ash Composite with Liquid Reactive Sintering Technology, Acta Metallurgical Sinica, pp. 465-470
35. Sudarshan, S. M. K., 2008, Dry Sliding Wear of Fly Ash Participle Reinforced A356 Al Composites, pp.349-360.
36. Joshi, R. C. and Lohtia, R. P., 1997, Fly Ash in Concrete Production, Properties and Uses, Gordon and Breach Science Publishers, Amsterdam, pp.1-47.
37. Milan Dvořák, New Methods Testing of Adhesion of the Coating to Sheet Metal by Bending, Emil Schwarzer, Faculty of Mechanical Engineering, Brno University of Technology, Brno, Czech Republic; 2 Fritzmeier Ltd., Vyškov, Czech Republic.
38. N.E., 1999, Mechanical behavior of materials: Engineering methods for deformation, fracture and fatigue, 2nd edition, Prentice Hall.
39. Askeland, D. R, Fulay P.P. and Wright W.J., 2010, The science and Engineering of Material, 6th ed, Cengage learning, Publisher ,Global Engineering :Christopher M. Shortt, Printed in the united states of America.

40. Bonforte J. M. and Monmoth S., 2001, Rubber and Plastics Corp, The joy of rubber and plastic, pp.1-34.
41. Lim G.T., Wong M.H., Reddy J.N., and Sue H.J., 2005, An integrated approach to-wards the study of scratch damage of polymer, Journal of Coatings Technology and Research.
42. Van Den Bosch M.J., Schreurs P. L. G., and Geers M. G. D., 2008, Identification and characterization of delamination in polymer coated metal sheet, Journal of the Mechanics and Physics of Solids, pp. 3259-3276.
43. Bunshah, Roitan F., 1994, Handbook of Deposition Technologies for Films and Coatings: Science, Technology and Applications, second edition. Materials science and process technology series. Park Ridge, N.J.: Noyes Publications.
44. Groover M.P., 2004 Fundamentals of Modern Manufacturing: Materials, Processes, and Systems, John Wiley & Sons, New York, NY.
45. Hutchings I.M. and Arnold E., Tribology: Friction and Wear of Engineering Materials, Elsevier Limited, London, UK, 16th edition.
46. Browning R.L., Lim G.T., A. Moyse, H.J. Sue, Chen H., and Earls J.D., 2006, Quantitative evaluation of scratch resistance of polymeric coatings based on a standardized progressive load scratch test," Surface and Coatings Technology, pp. 2970-2976.
47. Chaowasaako T., Sombatsompop N., 2007, Mechanical and morphological properties of fly ash/epoxy composites using of thermal and microwave curing methods, Composites Science and Technology.
48. Josepn C. D., 2003, Experimental measurement and finite element simulation of spring back in stamping Aluminum alloy sheets for auto-body panel application, M.Sc. thesis, Mississippi State University, Department of Mechanical Engineering.
49. Nakasone Y. and Yoshimoto S., 2006, Engineering Analysis with ANSYS software, Department of Mechanical Engineering, Tokyo University of Science.